UNIVERSITY OF CALIFORNIA, SAN DIEGO

Effects of Matrix Rigidity on Endothelial Cell Fate

A Dissertation submitted in partial satisfaction of the

requirements for the degree Doctor of Philosophy

in

Bioengineering

By

Joann May Chang

Committee in charge:

Professor Shu Chien, Chair
Professor Sylvia Evans
Professor Wayne Giles
Professor Joan Heller-Brown
Professor Lanping Amy Sung

2009

The Dissertation of Joann May Chang is approved, and it is acceptable in quality and form for publication on microfilm:

Chair

University of California, San Diego

2009

EPIGRAPH

You've got to say, "I think that if I keep working at this and want it badly enough I can have it." It's called perseverance.

Lee Iacocca

Basic research is what I'm doing when I don't know what I'm doing.

Wernher von Braun

A man who dares to waste one hour of time has not discovered the value of life.

Charles Darwin

It is not so much that I have confidence in scientists being right, but that I have so much in nonscientists being wrong.

Isaac Asimov

TABLE OF CONTENTS

LIST OF ACRONYMS

7-AAD	7-amino-actinomycin D
AFM	atomic force microscopy
ANOVA	analysis of variance
APS	ammonium persulfate
BAEC	bovine aortic endothelial cell
bFGF	basic fibroblast growth factor
BSA	bovine serum albumin
cDNA	complementary deoxyribonucleic acid
dH_2O	deionized water
DMEM	Dulbecco's Modified Eagle Medium
DMSO	dimethyl sulfoxide
DNA	deoxyribonucleic acid
E2F	E2 transcription factor
EC	endothelial cell
ECL	enhanced chemiluminescence
ECM	extracellular matrix
EDTA	ethylenediaminetetraacetate
EGF	epidermal growth factor
eNOS	endothelial nitric oxide synthase
ERK	extracellular signal-regulated kinase
FAK	focal adhesion kinase
FBS	fetal bovine serum

FSC	forward scatter channel
FITC	fluorescein isothiocyanate
GSK-3β	glycogen synthase kinase-3β
HEPES	4-(2-hydroxyethyl)-1-piperazineethanesulfonic acid
LDL	low density lipoprotein
MDM2	murine double minute oncogene
NaCl	sodium chloride
NaOH	sodium hydroxide
$NaVO_4$	sodium orthovanadate
NF-κB	nuclear factor *kappa* B
NIH	National Institutes of Health
PAG	polyacrylamide gel
PAGE	polyacrylamide gel electrophoresis
PECAM	platelet endothelial cell adhesion molecule
PI	propidium iodine
PI3K	phosphoinositide 3-kinase
PKB	protein kinase B
PMSF	phenylmethylsulphonyl fluoride
PS	phosphatidylserine
RGD	arginine glycine aspartic acid
RPTPα	receptor-like protein-tyrosine phosphatase alpha
RT	room temperature
SH	Src homology

SSC	side scatter channel
SEM	standard error of means
SDS	sodium dodecyl sulfate
Sulfo SANPAH	sulfosuccinimidyl 6-(4'-azido-2'-nitrophenylamino) hexanoate
TBSt	tris-buffered saline with 0.1% tween20
TEMED	tetramethylethylenediamine
UCSD	University of California, San Diego
UV	ultra violet
WT	wild type

LIST OF FIGURES

CHAPTER II

CHAPTER III

ACKNOWLEDGEMENTS

I would like to express my greatest gratitude to my advisor, Dr. Shu Chien, for his constant encouragement, wonderful support, and invaluable guidance. His vast wealth of knowledge has always awed and inspired me to learn more and strive to be a better scientist. He always made time to meet and discuss my project no matter how busy he was with travel or meetings. I am very grateful for his help and dedication to me. I feel very privileged to have worked with Dr. Chien and learned under his tutelage.

I wish to also extend my gratitude to Dr. Julie Li who helped me on a multitude of levels. Her door was always open and we could always discuss the good, the bad, and the ugly. Her guidance and knowledge helped me immensely throughout my graduate career and I will always appreciate it.

I would like to thank Drs. Shu Chien, Lanping Amy Sung, Wayne Giles, Sylvia Evans, and Joan Heller-Brown for serving as the members of my committee. I thank you for your expertise and time spent on my research.

I owe a debt of gratitude to past and current members of the Chien laboratory for supporting me, providing technical assistance, advice, and laughter. I want to especially thank Dr. Peter Wang, Dr. Jason Haga, Dr. Ian Lian, Dr. Angela Young, Dr. Sung Sik Hur, Dr. Troy Hornberger, Dr. Daniel Fero, Leona Flores, Mark Wang, Dayu Teng, Amy Hsieh, Phu Nguyen, Jennifer Chun, Suli Yuan, and Jerry Norwich.

My Ryuei Ryu Okinawan karate-do family here at UCSD has been a big source of support for me in my graduate career. I wish to thank them from the bottom of my heart for cheering me on to the finish line and providing a great source of stress relief. I have never met a better group of friends or karate practitioners.

Last, but definitely not least, I would like to say a big thank you to my family and husband, Francisco, for their undying support. I would have never made it without all your love, encouragement, and faith in me. All of you helped me see the light at the end of the tunnel and the bonds of family have never been stronger. As a postscript thank you, I would like to thank my twin baby girls for not making an early surprise entry into the world as I completed this dissertation.

CURRICULUM VITAE

EDUCATION

Ph.D., Bioengineering	University of California, San Diego June 2009
M.S., Bioengineering	University of California, San Diego December 2003
B.S., Materials Science and Engineering	University of Arizona May 2001

TEACHING EXPERIENCE

Teaching Assistant Consultant, University of California, San Diego 2004-2007
Center for Teaching Development

- Observed Teaching Assistants to provide feedback on their performance and assisted them in developing and utilizing active teaching skills.

Head Teaching Assistant Liaison, University of California, San Diego 2006-2007
Department of Bioengineering

- Assisted head teaching assistant with workshops to prepare graduate students for their teaching assistant assignments.

Assistant Instructor, University of California, San Diego Summer 2004
Academic Connections

- Developed a lecture on cell signaling to teach high school students interested in Bioengineering and taught them how to prepare laboratory reports for presentation in a group setting.

Teaching Assistant, University of California, San Diego 2002-2004

- Assisted in the instruction of Introduction to Bioengineering Physiology (BE 140B) and Continuum Mechanics (BE 110) courses.

Tutor, University of Arizona, Tucson 1999-2001
Math and Science Learning Center, TRIO program

- Conducted group study sessions for specific courses for a small group of students in the same course or in a one-on-one environment. Certified Master Tutor through the National College of Reading and Learning Association.

PUBLICATIONS

Wang Y, **Chang J**, Chen KD, Li S, Li JY, Wu C, Chien S. Selective adapter recruitment and differential signaling networks by VEGF vs. shear stress. Proc Natl Acad Sci U S A. 2007 May 11

Wang Y, **Chang JM**, Li YC, Li YS, Shyy JY, Chien S. Stress and VEGF Activate IKK via Flk-1/Cbl/Akt Signaling Pathway. Am J Physiol Heart Circ Physiol. 2003 Oct 9

Sajiv Boggavarapu, **Joann Chang**, and Dr. Paul Calvert. A test for mineralization for calcium salts using agarose hydrogels. Materials Science and Engr. C, 2000, 47 – 49.

AWARDS RECEIVED

- Poomi Jensen Scholarship, May 2006
- National Institutes of Health Training Grant, September 2001 – September 2003

ABSTRACT OF THE DISSERTATION

Effects of Matrix Rigidity on Endothelial Cell Fate

by

Joann May Chang

Doctor of Philosophy in Bioengineering

University of California, San Diego, 2009

Professor Shu Chien, Chair

Atherosclerosis, which involves arterial hardening, is a common cause of cardiovascular diseases. Alterations in the microenvironment of the arterial walls in diseased vessels may lead to significant changes in endothelial function. The extracellular matrix (ECM) is a vital component of the cellular microenvironment and has been shown to play an important role in endothelial cell (EC) function. The aim of the current study is to investigate the role played by matrix rigidity in the modulation of EC function and the underlying molecular signaling mechanisms.

Using a synthetic substrate with a range of stiffness that may mimic the various states of cellular microenvironment, my results show that stiff matrices increased EC

proliferation, while softer matrices decreased proliferation without the accompaniment of apoptosis. In addition to changes in proliferation, EC spreading area increased with the increase in rigidity of the matrix. Although ECs on stiffer matrices had larger cell areas than ECs on softer matrices, comparisons of the ellipticity ratio indicates there are no differences in cell shape.

To examine the regulatory events between matrix rigidity and EC proliferation, an RGD blocking peptide was used to block integrin interactions between the ECM and ECs. The RGD peptide significantly decreased proliferation of cells on the hard matrix, indicating the role of integrins in mediating the hard matrix-induced EC proliferation. Src and Akt phosphorylations were significantly lower on stiff matrix than on the soft one. The RGD peptide increased the phosphorylation levels of Akt and Src of ECs on the hard matrix to levels comparable to those on the soft matrix. Increasing the Akt and Src activities in ECs by transfecting with a constitutively active Akt construct or a wild-type Src cDNA caused the reversion of EC proliferation on the stiff matrix. These results indicate that ECs interact with their matrix through the integrin-Src/Akt pathway to regulate their proliferation. These findings on the effects of matrix rigidity on EC proliferation and their regulation by the integrin-Src/Akt pathway provide new insights for the understanding of EC-matrix interaction in health and disease.

Chapter I

Introduction

I.A. Arterial Stiffness

Cardiovascular disease is a leading cause of mortality, morbidity, and disability of men and women in industrialized nations. There are many ailments that fall under the category of cardiovascular disease; they include but are not limited to stroke, coronary artery disease, heart attacks, hypertension, and atherosclerosis. An important underlying cause of most cardiovascular diseases is atherosclerosis, i.e., the hardening of the arteries. Atherosclerosis is a chronic vascular inflammatory disease that involves the abnormal accumulation of low density lipoproteins, macrophages, other cellular components, and connective tissue within the artery wall. These accumulations lead to plaque formation that narrows the lumen, hardens the artery, and eventually occludes blood flow through the vessel. As the name of atherosclerosis implies, there is an increase in stiffness of the vessel wall.

It is well known that the elastic modulus of the artery increases with age. It has also been demonstrated that vascular disease, hypertension, diabetes, and insulin resistance can lead to an increase in arterial stiffness [Atabek et al., 2006; Liao et al., 1999; Wuyts et al., 1995; Danias et al., 2003]. Alterations in the microenvironment of the arterial walls can be observed in hypertensive vessels where smooth muscle cells (SMCs) begin to proliferate, undergo hyperplasia and hypertrophy, and collagen synthesis increases. The endothelium plays a major role in regulating vascular functions. There is evidence that atherogenesis is related to an accelerated endothelium turnover, with an increased endothelial cell (EC) proliferation and disruption of cell junctions, which in turn causes leakage and contributes to lesion formation [for review see Chien 2003]. Degeneration of the artery wall continues to progress due the increases in wall

tension when the artery dilates. These factors contribute to the increase in wall thickness and reduced vascularity of the vessel and cause the intima to be more susceptible to atherosclerosis [Arnett et al., 1994], thus perpetuating a vicious cycle that leads to the formation of fibrous caps with the vessel losing its ability to dilate, altering its elasticity, and impeding blood flow [Ross, 1999].

How the mechanical properties of the artery regulate vascular cell functions and lead to the etiology and pathology of hypertension, atherosclerosis, and other vascular diseases have not been clearly established. A better understanding of how the endothelium responds to its microenvironment either through mechanical or chemical stimuli will aid in the elucidation of the atherosclerotic progression and hence the related cardiovascular diseases.

I.B. Extracellular Matrix

The cellular microenvironment is crucial to the homeostasis of cells within a tissue or organ. A vital component to the cellular microenvironment is the extracellular matrix (ECM), which is mainly composed of laminin, thrombospondin, fibronectin, collagen, vitronectin, tenascin, and various proteoglycans and glycosaminoglycans, which form an organized network in which cells attach themselves to their environment [Hay, 1981]. The ECM is a component of the cellular microenvironment for all cell types, but the spatial relationship and the exact composition of the ECM differ among cells of different tissues. It has been demonstrated that the ECM, via signaling through integrins, modulate gene and protein expressions and influence various cellular functions, such as morphology, growth, differentiation, and apoptosis [Adams et al., 1993;

Boudreau et al., 1999]. How cells become activated for each of these functions is dependent upon cellular interaction with their ECMs, as well as cellular responses to chemical or mechanical stimuli.

The family of integrins, which transmit signals between the cell and the ECM [Boudreau et al., 1999], is a major group of ECM receptors. The integrins are heterodimeric molecules composed of α and β subunits that are transmembrane receptors with cytoplasmic domains, which interact with the actin cytoskeleton and associated proteins, and the extracellular domains, which bind to the ECM. Integrins have been shown to play an important role in regulating EC proliferation and angiogenesis [Stromblad and Cheresh, 1996; Kobayashi-Sakamoto et al., 2008].

I.C. Extracellular Matrix Mechanics

There is an abundance of data that demonstrate the pivotal role the ECM plays in many cellular functions. Recently, there is an emergence of new data that suggest that changes in the mechanical properties of microenvironment can modulate cellular behavior and tissue function. Multiple systems have been developed to modify the matrix rigidity for studies with different cell types. Natural protein-based ECM gels can be derived from fibrin, collagen, agarose, or a mixture of laminin, collagen, and other proteins to form Matrigels. These are commonly formed into two- or three-dimensional substrates to control their rigidity. Synthetic substrates can also be derived from polyacrylamide gels (PAG), polyethylene glycol gels, silicone membranes, or micropatterned elastomer substrates [Georges et al., 2005; Peyton et al., 2007].

Most cells rely on their anchorage to a solid surface to maintain their viability. It has been shown that cells can sense their microenvironment and transmit forces to their surrounding substrate through their myosin-based contractility and cellular adhesions [Ingber, 2002]. Cells can respond to the changes in their surroundings through the reorganization of their cytoskeleton, thus adjusting the contractile forces they exert to the substrate and modifying their biological and mechanical behavior [Discher et al., 2005]. The examination of different cell types on varying matrices has shown a correlation between matrix rigidity and cellular morphogenesis, functions, and homeostasis, as well as disease processes [Halliday et al., 1995; Sieminki et al., 2004; Engler et al. 2004; Kusaka et al., 2000].

I.D. Matrix Rigidity and Cellular Behavior

The importance of the interactions between ECM mechanics and cells was first demonstrated by Harris and colleagues in 1981, where they examined NIH 3T3 fibroblast traction forces on distortable sheets of silicone rubber. Subsequently, Wang and colleagues developed the more quantitative beads-in-gel technique to show that fibroblast migration is dependent on ECM stiffness [1997]. Their work demonstrated the preference of fibroblasts to migrate from a soft matrix to a stiff matrix, and this new form of directed cell migration is referred to as durotaxis. Based on these studies, further analyses of fibroblast migration have been done on collagen gels to monitor the dynamics of stress fibers and focal adhesions [Halliday et al., 1995] and on PAG substrates to detect compliance-dependent changes in cytoskeletal adhesion and motility [Pelham et al., 1997].

Besides the research on fibroblasts, studies have also been performed to elucidate the role of mechanics of ECM in its interaction with many other cell types. For example, investigations have been performed to study the matrix rigidity-dependent formation of myotubes with myosin striations [Engler et al., 2004], and how ECM deposition by hepatic satellite cells located in the Disse leads to increase tissue stiffness in disease states [Maher et al., 1988]. Studies have also been performed to show that neurons have a higher success rate for nerve regeneration on soft matrices in comparison to hard matrices that mimic scars [Balgude et al.,2001], and that SMCs can sense subtle gradients in mechanical compliance [Wong et al., 2003] and can transition from its contractile phenotype to a synthetic phenotype based on the ECM composition, mechanical stress, and soluble factors [Thyberg, 1998; Thyberg et al., 1995]. The most intriguing finding is the recent report that directed stem cell differentiation can be modulated through matrix elasticities [Engler et al., 2006].

I.E. Extracellular Matrix Mechanics and Endothelial Cells

With the emergence in new findings on ECM mechanics and cellular mechanotransduction, there are increasing interests in the interaction of ECs with the ECM. Most of the early work emphasized capillary morphogenesis or tubulogenesis. Vernon et al. examined ECs on collagen gels and observed capillary morphogenesis on softer gels, whereas a decrease of the capillary network was seen on stiffer gels [1992]. Vailhe et al. also obtained similar findings on fibrin gels [1997]. Gooch's group demonstrated that the softer matrices allowed ECs to form long capillary-like tube structures, but on stiffer matrices ECs were more spread out with large lumens and less

branching. In regards to EC morphology, Yueng et al. observed an increase in projected cell area and circumference with increasing substrate stiffness [2005]. A more in-depth observation of EC attachment and spreading was conducted in a co-culture model with SMCs by Truskey's group. They found that the $\alpha_v\beta_3$-integrin aided ECs in only their attachment to SMCs, while the $\alpha_5\beta_1$-integrin aided ECs in attaching and spreading on top of SMCs [2007].

In summary, it is apparent that the ECM plays a pivotal role in regulating EC function. Studies in the current literature have provided a considerable amount of evidence that the ECM plays an important role in capillary morphogenesis, interactions with integrin, and EC morphology. However, there needs to be a more in-depth understanding of how ECs interact with the ECM, especially in relation to vascular functions such as proliferation.

I.F. Hypothesis and Objectives

The aim of this research is to study the effects of matrix rigidity on EC function. I hypothesize that EC proliferation is dependent on matrix rigidity, and that such dependence is mediated through integrins, Src, and Akt.

In Chapter II, the goal is to demonstrate that matrix rigidity modulates EC proliferation and cell spreading area. My results show that EC proliferation and cell spreading area increase with increasing matrix rigidity. In Chapter III, the goal is to investigate the mechanism by which matrix rigidity modulate EC proliferation. My results elucidate the important role that integrins play as mechanotransducers for the regulation of cell proliferation by matrix rigidity. Further, I show that Src and Akt are

important downstream signaling molecules that regulate the EC proliferation in response to the changes in matrix rigidity. In summary, my study demonstrates that the effects of matrix rigidity on cell proliferation and morphology are integrin-dependent and that Src and Akt play key roles in mediating the matrix rigidity-dependent EC proliferation.

Chapter II

The Effects of Matrix Rigidity on EC Proliferation and Spreading

II.A. Abstract

Polyacrylamide gels (PAGs) can be cross-linked to form gels of varying rigidities. By changing the relative concentrations of acrylamide and bis-acrylamide used in the formulation, gels with various Young's moduli were prepared to mimic a range of ECM rigidity for ECs to be seeded. Using these varying gel rigidities, I have demonstrated that matrix rigidity modulates EC proliferation and cell spreading area. An increase in matrix rigidity led to increases in EC proliferation and cell spreading area. I also have demonstrated that the decrease in cell density on softer matrices is attributable to a lower proliferation rate, and not accompanied by cell apoptosis. Furthermore, the ellipticity ratios of ECs are similar on stiff and softer matrices, indicating that the increase in EC area on stiffer matrices is not accompanied by a relative cell elongation.

II.B. Introduction

It has become increasingly recognized that mechanical stimuli can be as important as chemical stimuli in regulating cellular behaviors. The stiffness of materials to which cells adhere can play a pivotal role in modulating cell morphology, gene transcription, and growth rates. The recent increase in interest on how matrix rigidity affects cellular function has yielded multiple platforms onto which cells are seeded for investigations. Natural protein-based ECM gels derived from fibrin, collagen, agarose, or Matrigels (a mixture of laminin, collagen, and other proteins) are commonly used as substrates to control their rigidity. Synthetic substrates derived from ligand-coated polyacrylamide gels, polyethylene glycol gels, silicone membranes, or micropatterned elastomer substrates are also used for cellular studies [Georges et al., 2005; Peyton et al., 2007].

The theory that ECM mechanics plays an important role in cell function has gained momentum, and several groups have taken on studies on a variety of cells types that include fibroblasts, myocytes, neurons, liver-derived cells, stem cells, SMCs, and ECs. Among those cells, fibroblasts have been most intensively studied, which is in large part due to the work of Wang and colleagues, who first established the dependence of fibroblast migration on matrix stiffness in 1997. Thus far, the investigations of the effects of different matrix rigidities on ECs are limited to the characteristics of angiogenesis and capillary morphogenesis. It was observed that ECs formed capillary-like networks when seeded on softer collagen gels and that there was a decrease of this network formation on stiffer collagen gels [Vernon et al., 1992]. Vailhe et al. also observed a similar phenomenon on fibrin gels [1997]. In a 3-dimensional collagen gel, ECs were observed to form structural networks of tubes and lumens [Yang et al., 1999]

versus just capillary-like 2D-branch points, as observed by the previous two groups. Subsequent studies on EC angiogenesis examined integrins and growth factors that may promote this process on varying natural protein-based gels [Bach et. al., 1998; Montesano et. al., 1983; Ingber and Folkman, 1989].

Little work has been done in regards to the interplay between ECM mechanics and EC functions, either under physiological conditions or disease states. In examining EC morphology, Janmey's group was able to conclude that an increase in substrate rigidity increases the projected area and circumference of the cells [2005]. Wallace et al. were able to use a co-culture model to establish EC attachment and spreading on SMCs (presumably a softer substrate) through the $\alpha_5\beta_1$-integrin complex [2007]. The availability of the established synthetic and natural ECM platforms has made it possible to conduct further research into the interplay between the mechanics of ECM and ECs, especially in conditions that can mimic the hardening of the microenvironment such as atherosclerotic/hypertensive disease states.

The aim of this chapter is to elucidate the relationship between matrix rigidity and EC proliferation. By using different ratios of acrylamide and bis-acrylamide concentrations to form PAGs, I was able to construct matrices with varying rigidities to examine the EC proliferation responses as a function of this variable. In addition, the effects of matrix rigidity on EC apoptosis were also studied. Moreover, I examined whether the EC spreading areas on various matrix rigidities play a role in EC turnover. The results of this chapter demonstrate that matrix rigidity plays a significant role in modulating EC function and morphology.

II.C. Material and Methods

II.C.1. Cell Culture

The procedure to isolate bovine aortic endothelial cells (BAECs) was described by Gimbrone [1976]. Cell culture reagents were obtained from Invitrogen (Carlsbad, CA). The cells were cultured in DMEM containing 10% FBS (Omega Scientific, Tarzana, CA), 2 mM L-glutamine, 1 mM sodium pyruvate and 1% penicillin/streptomycin, and maintained in a humidified 5% CO_2-95% air incubator at 37^{o}C. To ascertain their origins, the cultured BAECs were stained with the EC marker von Willebrand factor. All experiments were conducted with BAEC cultures prior to passage 7.

II.C.2. Glass Slide Preparation

The glass microscope slides were chemically activated for covalent attachment of polyacrylamide based on a protocol previously established by Wang and Pelham (1997). The glass microscope slides (75 x 38mm, Corning) were passed over the flame of a Bunsen burner, coated with 0.1M NaOH for 5 min, rinsed in dH_2O, and allowed to dry. The slides were then coated with a layer of 3-aminopropyltrimethoxysilane (250 µL, Sigma-Aldrich Chemical, St. Louis, MO) for 5 min and repeatedly rinsed in dH_2O until no residues of the 3-aminopropyltrimethoxysilane remain. This was then followed by 30-min incubation in 0.5 % glutaraldehyde (8 % stock solution, Sigma-Aldrich Chemical) in PBS (Invitrogen, Carlsbad, CA) at room temperature. The glass microscope slides were thoroughly rinsed in dH_2O and allowed to dry.

II.C.3. Polyacrylamide Gel Preparation

Gel solutions were prepared using 5 – 10% acrylamide (40% w/v solution, Bio-Rad), 0.05 – 0.2% bis-acrylamide crosslinker (2% w/v solution, Bio-Rad), 1% HEPES (pH 8.5, EMD Biosciences), and degassed for 20 min to remove oxygen from the solutions. 0.02% APS and 20 μL TEMED were added to initiate polymerization. A 50 – 70 μm thick gel was formed, and the thickness was confirmed through the imaging of embedded fluorescent beads in the gel on an Olympus confocal microscope. The rigidities of the gel substrates were determined by Atomic Force Microscopy.

II.C.4. Mechanical Characterization of Gels Using Atomic Force Microscopy (AFM)

A Bioscope BS3-0 Atomic Force Microscope (Veeco, Woodbury, NY) was used to make indentations. Pyramid-shaped cantilevers DNP-10 and MLCT (Veeco) with spring constants of 0.6 and 0.5 N/m, respectively, were employed in the experiments.

The relationship between the loading force and indentation of various geometries was calculated by Sneddon [1965]:

$$F = \frac{2}{\pi} \bullet \frac{E}{1-\upsilon^2} \bullet \delta^2 \tan(\alpha) \qquad (1)$$

where F = force, E = Young's modulus, , υ = Poisson's ratio, δ = indentation, and α = opening angle of the cone.

The principle of the AFM characterization is based on a micro-cantilever equipped with a pyramid-shaped probe that is brought to the surface of the sample by a piezo motor. As the motor drives the cantilever further downward after the probe has

made contact with the surface of the sample, a force is exerted by the cantilever on the matrix.

This loading force at any given time is determined by Hook's law:

$$F = kd \qquad \textbf{(2)}$$

where k is the spring constant of the cantilever and d is the degree of bending. A corresponding force-deflection curve is then generated. The indentation in the soft material is measured by the difference of the motor distance z and laser deflection d.

$$\delta = z - d \qquad \textbf{(3)}$$

The Young's modulus E can be calculated using Equation 1, assuming the Poisson's ratio υ to be 0.45 and knowing the opening angle of the pyramid probe α is 35°. The force-deflection curve was obtained using the "Force Calibration Mode" with an indentation distance of 2 – 3 μm in the z direction.

In order to have accurate values for the spring constants, the cantilevers were calibrated using CLFC calibration cantilevers (Veeco) with precise dimensions and spring constant, according to the instructions of the manufacturer. Briefly, the tested cantilever is aligned on top of the calibration cantilever. The deflection sensitivity (S_{ref}) was obtained in the force mode by tracing the slope of the curve. Five S_{ref} values were obtained for gels with different rigidities, and the mean value was determined. The tested cantilever was moved on top of the glass surface to determine the mean S_{hard}.

The offset ΔL was found by estimating the distance from the tip of the probe to the edge of the calibration cantilever. The spring constant k of the tested cantilever can be calculated from:

$$k = k_{ref}\left(\frac{S_{ref}}{S_{hard}} - 1\right)\left(\frac{L}{L - \Delta L}\right)^3 \qquad (4)$$

where k_{ref} is the reference spring constant; L is 400 μm, the length of the calibration cantilever; and ΔL is the offset length. The data were then converted to an Excel format. From Equations 2 and 3, the Force and indentation δ can be calculated.

A fit of Equation 1 was applied to the force vs. δ curve using the MATLAB software. The elastic constant E was then calculated from the resultant coefficient from Equation 1.

II.C.5. Fibronectin Coating and Cell Seeding

The prepared PAGs on the glass microscope slides were coated with sulfo-SANPAH (Bioworld) and treated with UV light (254 nm) for 7 min, twice, and rinsed clean with 50 mM HEPES (pH 8.5). The gels were then coated with 1.5 μg/cm^2 of fibronectin (0.1% solution, Sigma-Aldrich Chemical), diluted in PBS, and allowed to incubate overnight at 4^{o}C.

The gels were sterilized under a UV lamp (254 nm) for 15 min, rinsed with PBS, and incubated with FBS complete media for 1 hr at 37^{o}C before cell seeding. The cells from one 10-cm diameter Petri dish were used to seed 5 PAG slides. BAECs were allowed to adhere to the gels for 1 hr before the addition of 14 mL of FBS complete media.

II.C.6. Cell Proliferation Assay

Bromodeoxyuridine (BrdU) incorporation was utilized to assess cell proliferation. BrdU is a synthetic nucleoside, which is an analog of the DNA precursor thymidine. In cells that are entering or progressing through the S phase of the cell cycle, BrdU substitutes for thymidine in newly synthesized DNA and can be detected using a BrdU antibody.

Quantitative data were acquired using a two-colored flow cytometric analysis method. With the use of a BrdU flow kit (BD Pharmingen, San Diego, CA), BrdU (10 μM) was incorporated into ECs during the 23rd hr of a 24-hr culture on various matrix rigidities. The cells were subsequently fixed and processed according to the manufacturer's protocol. After 1 hr of DNase treatment at 37^{o}C, the cells were incubated with anti-BrdU conjugated with Alexa 488 and a DNA content staining agent, 7-amino-actinomycin D (7-AAD). A BD FACScan flow cytometer was used in conjunction with the BD CellQuest software to analyze the cell samples. The phases in the cell cycle: G_0/G_1 phase, G_2 + M phase, and S phase, were identified within the cell population of each sample and categorized into distinct quadrants mapped out by the CellQuest software. Further quantification of the cell numbers in each quadrant was done by the CellQuest analysis tool.

II.C.7. Cell Apoptosis Assay

Annexin V staining assay was used to assess cell apoptosis. One of the earliest features of an apoptotic cell is the flip of the plasma membrane. The membrane phospholipid phosphatidylserine (PS) in apoptotic cells translocate from the inner to the

outer leaflet of the plasma membrane. This translocation exposes the PS to the exterior environment and allows the binding of Ca^{2+}-dependent phospholipid-binding protein, Annexin V. Thus, this assay is an efficient and effective tool in assessing cells that are apoptotic. Quantitative data were obtained through the use of the Annexin V kit (BD Biosciences, San Diego, CA), which enabled a two-color flow cytometric analysis. BAECs on the PAGs were washed once with PBS and trypsinized (1x trypsin, Invitrogen, Carlsbad, CA), collected in 15-mL centrifuge tubes, and spun down at 3000 g for 3 min. The supernatant was aspirated off, and the pellet was washed twice with 2 mL of binding buffer. After the second wash, the pellet was resuspended in 100 μL of binding buffer. Five μL of fluorescein isothiocyanate (FITC)-conjugated Annexin V and 5 μL of propidium iodine (PI) (Sigma) were added to the resuspended cells and allowed to incubate at room temperature in the dark for 15 min. Stained cells were immediately used for flow cytometry analysis. Cells were separated into apoptotic or live cell quadrants, and the quantified cell numbers were generated by the CellQuest analysis tool.

II.C.8. Cell Elongation and Ellipticity Ratio Quantification

BAECs were seeded on glass and PAGs prepared at 10/0.02, 8/0.1, and 5/0.05 (% acrylamide / % bis-acrylamide) compositions. The cells were allowed to adhere for 24 hr, and phase images taken at the end of the culture period with an Olympus inverted microscope using a 10x objective and the Simple PCI image acquisition software. Using the Metamporh 6.3r6 software (Molecular Devices), the x- and y-axes of the images were adjusted to measure 0.641 μm per pixel, a clustered area of 20 cells were outlined and selected, and the long and short axes were measured. The ellipticity ratio was calculated

by dividing the long axis by the short axis. Data are representative of four different experiments (N=4).

II.C.9. Cell Area Quantification

BAECs were seeded on glass and PAGs at 10/0.02, 8/0.1, and 5/0.05 compositions. The cells were allowed to adhere for 24 hr, and phase images taken at the end of this period with an Olympus inverted microscope using a 10x objective and the Simple PCI image acquisition software. The 2-dimensional areas of individual cells were quantified based on a converted pixel area to micron area format, using the NIH Image J. Clustered areas of 25 cells were outlined and selected for area measurement. Pictures are representative of four separate experiments (N=4).

II.C.10. Cell Count Quantification

Phase images were taken of BAECs seeded on glass and PAG 10/0.2, 8/0.1 and 5/0.05 substrates after 24 hr of culturing. Images were taken using a 10x objective on the Olympus inverted microscope using the Simple PCI image acquisition software. All cells were counted in each image field and were averaged from 12 different fields.

II.C.11. Statistical Analysis

Data was analyzed by one-way ANOVA to test the differences between multiple groups, followed by the Dunnett's post hoc test using the JMP7 software (S.A.S Institute Inc., Cary, NC) to determine which groups differ through pair-wise comparisons.

Results were expressed as mean ± SEM from at least 3 independent experiments. * *P* values < 0.05 were considered to be statistically significant.

II.D. Results

II.D.1. Matrix Rigidity Modulates EC Proliferation

Pelham et al. [1997] first described the use of PAGs to study the effects of matrix rigidity on NIH 3T3 fibroblasts. The rigidity of the PAG sheets was characterized by stretching them with a known downward force created by binder clips and measuring the change in length. The Young's modulus was calculated according to the equation: $Y = (F_{\perp}/A)/(\Delta l/l)$. To test the rigidity of the PAGs constructed in the lab, AFM was utilized and calculations outlined in Section II.C.4 were implemented to calculate the Young's modulus. As shown in Figure II.1, PAG 10/0.2, 8/0.1, and 5/0.05 have Young's moduli of 10.10, 4.1, and 0.66 kPa, respectively. These moduli are relatively small in comparison to glass, which has a Young's modulus of 60 GPa [Crew, 1919].

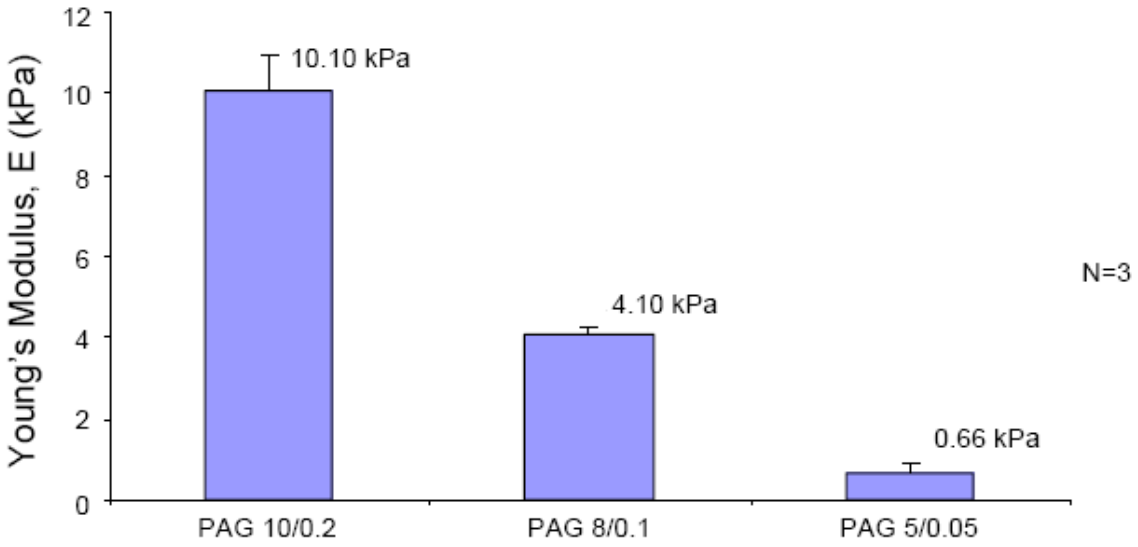

Figure II.1. Young's Moduli of Polyacrylamide Gels. The Young's modulus of the PAGs was measured by AFM (N=3).

With the established Young's moduli of the PAGs, BAECs were seeded onto the gels for 24 hr, and cell proliferation rate was examined by using the BrdU incorporation assay as described in Section II.C.6. Flow cytometric analysis was performed to obtain quantitative results of the cell cycle progression. The light scattering properties of the cell as it passes through the flow cytometry laser is shown in the upper left plot of Figure II.2.i. The x-axis represents the forward scatter channel (FSC) that detects the low angle, scattered light, which is proportional to the cell size. The y-axis is the side scatter channel (SSC) that detects high angle, scattered light, which is proportional to cell granularity and internal complexity. The FSC versus SSC plot shows that the BAECs in the experimental sample had little change in granularity and was rather uniform in size. The upper right plot (Fig. II.2.i) charts cells passing through the FL1 channel (emission 520 nm), which detects Alexa 488 anti-BrdU signals, and the FL3 channel (emission 690 nm), which detects 7-AAD signals. The plot logs 10,000 cell counts to determine statistical significance and the BD CellQuest software allows me to use the "Region Gates Calculation" to separate out the cell populations that have been stained with different levels of BrdU incorporation and total DNA content. The R1 gate encompassed cells in the sub-G_0/G_1 phase, where cells were negative for BrdU incorporation and had low levels of total DNA content. Cells that had low levels of BrdU incorporation and total DNA content represented the G_0/G_1 phase and are depicted in R2. R3 represents the G_2 + M phase where cells contained newly synthesized DNA, and therefore there was a low BrdU incorporation and a higher 7-AAD stained total DNA content. R4 represents cells that had active DNA synthesis in the S phase, so there was a high level of BrdU

incorporation and moderate levels of total DNA content. The lower left plot of Fig. II.2.i displays the cell count versus the FL1 channel, which represents BrdU-negative cells (low BrdU signal) versus BrdU-positive cells (high BrdU signal). The lower right plot displays the cell count versus the FL3 channel and represents cells in the range of total DNA content. All these plots combined provide a quantitative analysis of the cell cycle.

Figures II.2.i-iv illustrate a high percentage of ECs proliferating (S-phase) on the glass substrate and a progressive decrease in proliferation with decreasing PAG rigidities. The lowest cell proliferation occurred on the PAG 5/0.05 substrate as most of the cells shifted to the quiescent G_0/G_1 phase (Fig. II.2.iv). Fig. II.3 displays the statistical analysis of the results. Cells seeded on glass had the highest percentage of cells proliferating in S-phase (33.48 ± 2.18 %), and this percentage decreased with PAG 10/0.2 (31.22 ± 0.98 %), PAG 8/0.1 (23.81 ± 1.74 %) and PAG 5/0.05 (14.08 ± 1.01 %). The ECs seeded on soft PAG 5/0.05 showed a significant 2.2-fold decrease in S-phase when compared with those on hard PAG 10/0.2.

These flow cytometric results demonstrate that the matrix rigidity has a profound influence on EC proliferation. Harder matrix rigidities such as glass and PAG 10/0.2 led to augmented cell proliferation rate, while the softer matrix (PAG 5/0.05) showed a low cell proliferation rate. These findings provide a foundation for further investigations on the mechanisms by which matrix rigidities modulate EC functions.

Glass

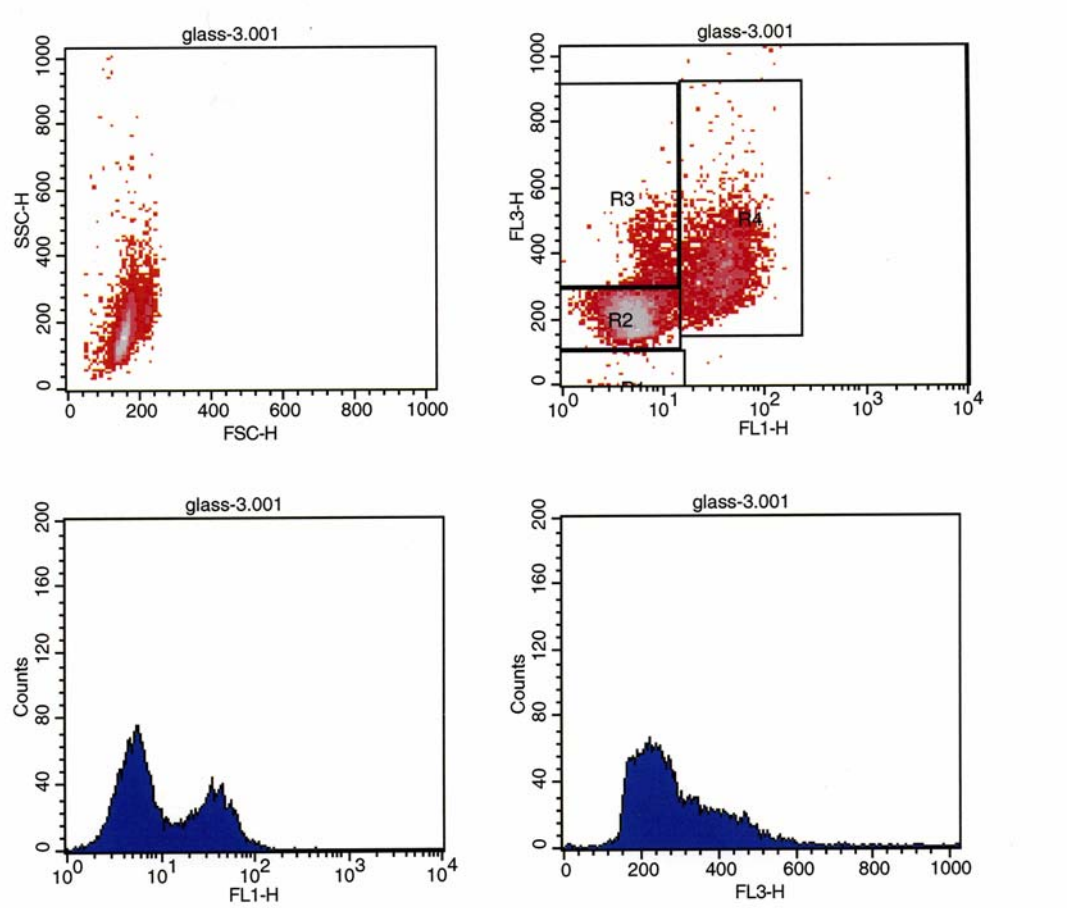

Region Statistics

File: glass-3.001
Sample ID: glass-3
Tube:
Acquisition Date: 25-Mar-08
Gated Events: 10000
X Parameter: FL1-H (Log)

Log Data Units: Linear Values
Patient ID:
Panel:
Gate: No Gate
Total Events: 10000
Y Parameter: FL3-H (Linear)

Region	Events	% Gated	% Total	X Mean	X Geo Mean	Y Mean	Y Geo Mean	Px,Py
R1	17	0.17	0.17	4.42	3.90	41.29	28.78	3, 5
R2	5552	55.52	55.52	5.32	4.94	215.66	212.13	3, 5
R3	916	9.16	9.16	8.09	7.65	394.33	387.53	3, 5
R4	3407	34.07	34.07	38.33	34.93	367.94	356.30	3, 5

Figure II.2.i. Flow cytometric analysis of the cell cycle for cells seeded on glass. R1, R2, R3, and R4 region gates denote cells in sub G_0/G_1, G_0/G_1, G_2 + M, and S-phases, respectively. Cells seeded on glass exhibit a higher percentage of cells in S-phase proliferation at about 34% (statistics table given below the graphs).

PAG 10/0.2

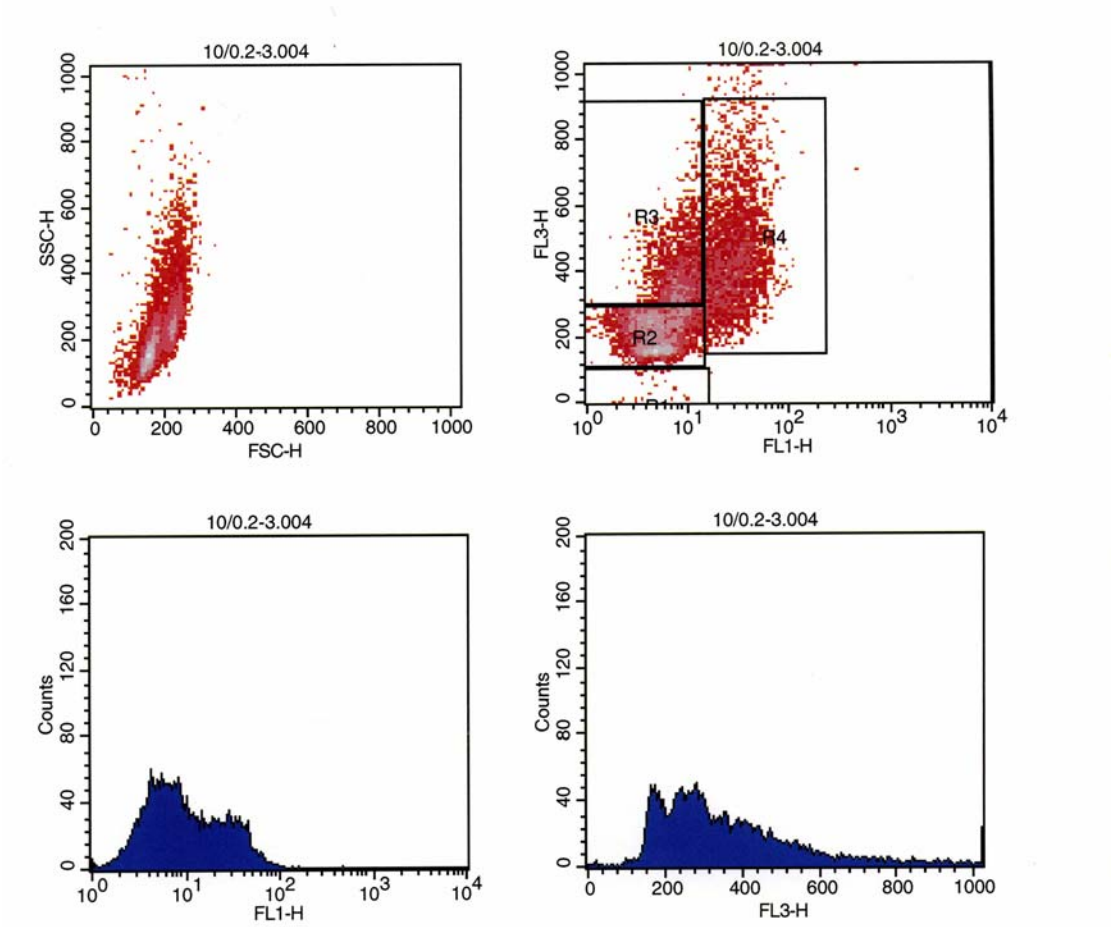

Region Statistics

File: 10/0.2-3.004
Sample ID: 10/0.2-3
Tube:
Acquisition Date: 25-Mar-08
Gated Events: 10000
X Parameter: FL1-H (Log)

Log Data Units: Linear Values
Patient ID:
Panel:
Gate: No Gate
Total Events: 10000
Y Parameter: FL3-H (Linear)

Region	Events	% Gated	% Total	X Mean	X Geo Mean	Y Mean	Y Geo Mean	Px,Py
R1	24	0.24	0.24	3.90	3.39	47.88	30.82	3, 5
R2	4498	44.98	44.98	5.36	4.84	218.62	213.95	3, 5
R3	2167	21.67	21.67	8.50	8.05	400.66	392.34	3, 5
R4	3014	30.14	30.14	29.34	27.12	448.03	425.47	3, 5

Figure II.2.ii. Flow cytometric analysis of the cell cycle for cells seeded on PAG 10/0.2. Cells seeded on PAG 10/0.2 exhibit a slight decrease in S-phase proliferation at about 30% compared to the 34% of cells seeded on glass (Statistics shown in Fig. II.3).

PAG 8/0.1

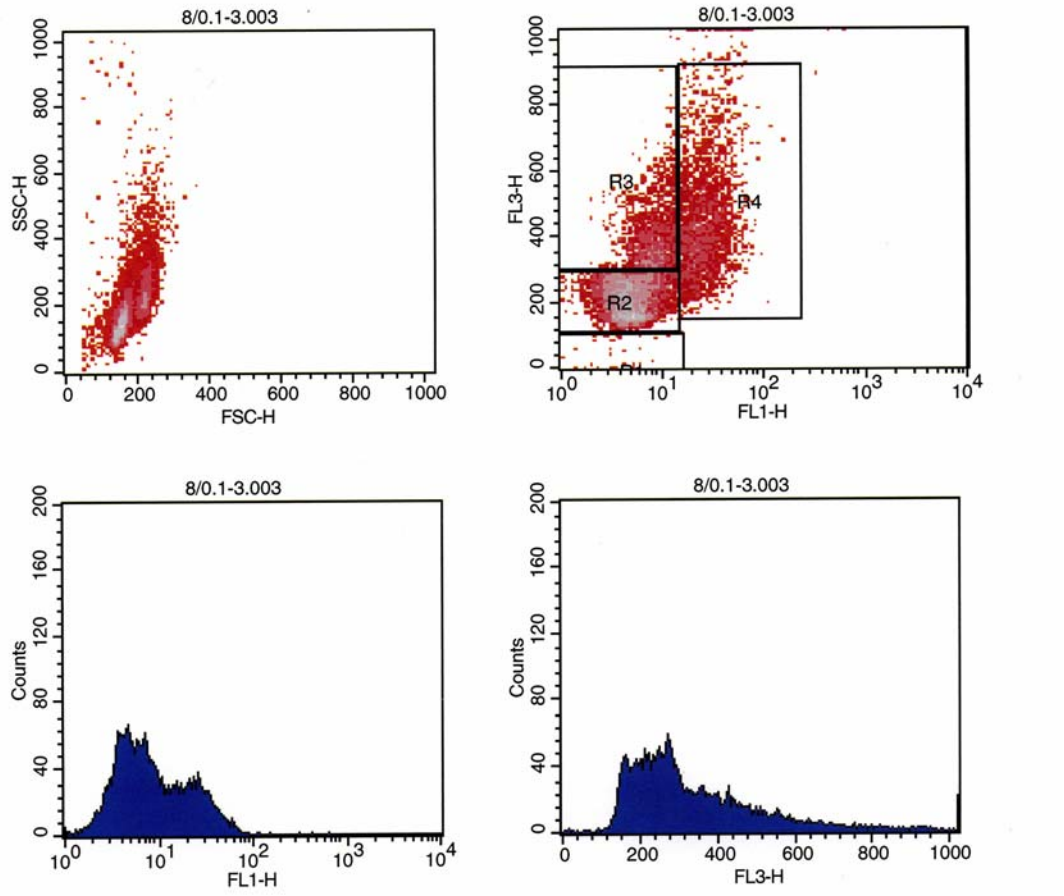

Region Statistics

File: 8/0.1-3.003
Sample ID: 8/0.1-3
Tube:
Acquisition Date: 25-Mar-08
Gated Events: 10000
X Parameter: FL1-H (Log)

Log Data Units: Linear Values
Patient ID:
Panel:
Gate: No Gate
Total Events: 10000
Y Parameter: FL3-H (Linear)

Region	Events	% Gated	% Total	X Mean	X Geo Mean	Y Mean	Y Geo Mean	Px,Py
R1	26	0.26	0.26	3.47	3.02	39.85	25.96	3, 5
R2	5135	51.35	51.35	5.14	4.68	217.02	212.30	3, 5
R3	1961	19.61	19.61	8.39	7.91	405.40	396.57	3, 5
R4	2624	26.24	26.24	26.95	25.17	446.13	423.13	3, 5

Figure II.2.iii. Flow cytometric analysis of the cell cycle for cells seeded on PAG 8/0.1. Compared to glass and PAG 10/0.2, cells seeded on PAG 8/0.1 have less cells in S phase proliferation at about 26% (Statistics shown in Fig. II.3).

PAG 5/0.05

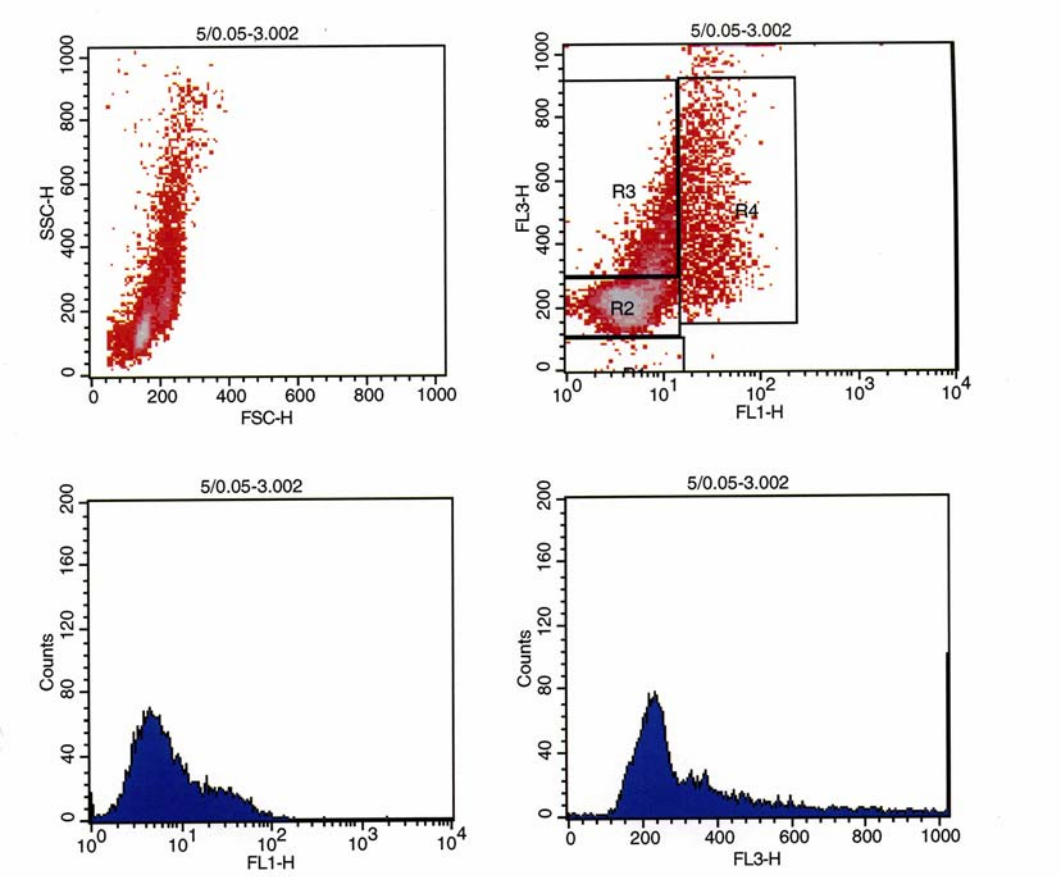

Region Statistics

File: 5/0.05-3.002
Sample ID: 5/0.05-3
Tube:
Acquisition Date: 25-Mar-08
Gated Events: 10000
X Parameter: FL1-H (Log)

Log Data Units: Linear Values
Patient ID:
Panel:
Gate: No Gate
Total Events: 10000
Y Parameter: FL3-H (Linear)

Region	Events	% Gated	% Total	X Mean	X Geo Mean	Y Mean	Y Geo Mean	Px,Py
R1	28	0.28	0.28	4.22	3.50	47.11	31.79	3, 5
R2	5989	59.89	59.89	4.63	4.25	217.65	214.45	3, 5
R3	1909	19.09	19.09	8.67	8.23	408.94	399.05	3, 5
R4	1642	16.42	16.42	29.61	26.82	487.84	453.23	3, 5

Figure II.2.iv. Flow cytometric analysis of the cell cycle for cells seeded on PAG 5/0.05. Compared to glass (34%), PAG 10/0.2 (30%) and PAG 8/0.1 (26%), cells seeded on PAG 5/0.05 have the least percentage of cells in S phase proliferation at about 16% (Statistics shown in Fig. II.3).

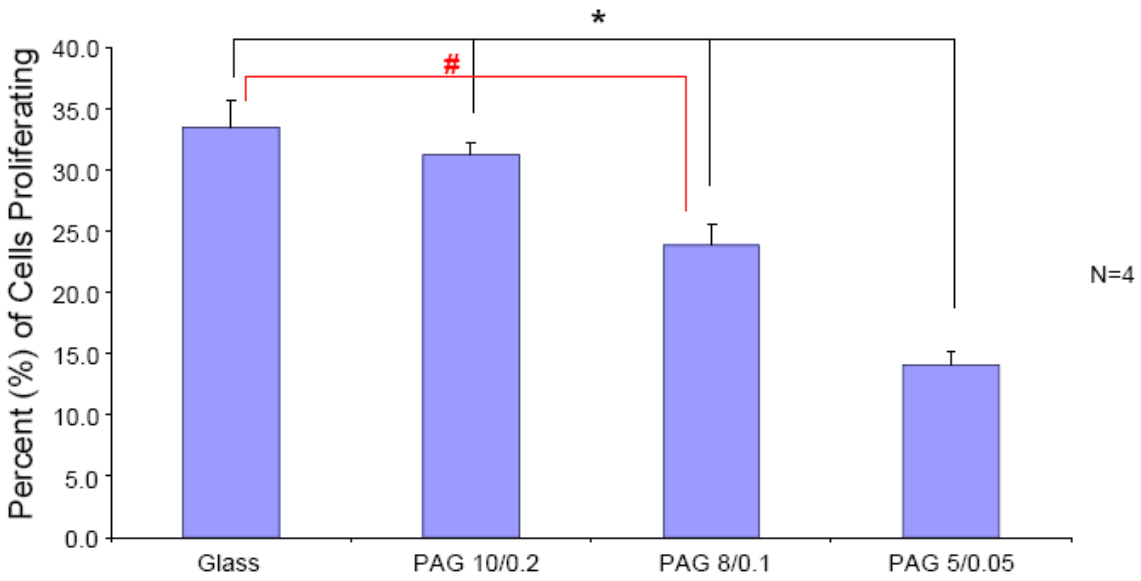

Figure II.3. Flow cytometric cell cycle analysis of cells in active DNA synthesizing S-phase. This bar graph demonstrated the results of cells in S phase from the preceding four figures. EC cell cycle analysis derived from flow cytometry data. Cells seeded on glass show the highest percentage of cells in S-phase, while the lowest percentage is present in cells seeded on the softest matrix, PAG 5/0.05. * $P < 0.05$ when compared to PAG 5/0.05. # $P < 0.05$ when compared to glass. Error bars represent SEM.

II.D.2. Decrease in Cell Proliferation on Soft Matrix Was Not Accompanied by Apoptosis

Flow cytometric analysis from the preceding section demonstrated that a decrease in matrix rigidity led to a decrease in EC proliferation. I tested whether this decrease was accompanied by a change in cell apoptosis. BAECs were seeded onto the glass, PAG 10/0.2, 8/0.1, and 5/0.05 substrates for 24 hr and collected for Annexin V analysis. Quantitative analysis was performed using flow cytometry and the Annexin V kit mentioned in Section II.C.7. The upper left plot of Fig. II.4.i charts the cell count versus the FL1 channel (emission 490 nm), which represents the cells within the range of FITC-stained Annexin V. The middle plot charts the cell count versus the FL3 channel (emission 451 nm) and represents cells within the range of total DNA content stained by PI. The right plot charts the FL1 channel (FITC Annexin V) versus the FL3 channel (PI). The plot logs 10,000 cell counts to determine statistical significance, and the BD CellQuest software allocates the cells into four possible quadrants. The lower left (LL) quadrant identifies cells that are viable, and FITC Annexin V and PI negative. The lower right (LR) quadrant identifies cells undergoing apoptosis and is FITC Annexin V positive and PI negative. The upper left (UL) quadrant is cells that are dead and FITC Annexin V negative and PI positive. The upper right (UR) quadrant identifies cells that are both FITC Annexin V and PI positive, which indicates that they are in the end stage of apoptosis.

Fig. II.4.i illustrates the high percentage of viable cells seeded on the glass substrate with a very low percentage of cells that were apoptotic. Figs. II.4.ii-iv display the results for the remaining PAG substrates. All demonstrate high percentages of viable

cells. Fig. II.5 displays the statistical analysis of the results. Comparison of the percentages of viable and apoptotic cells, respectively, on glass (91.0 ± 1.1 % and 0.89 ± 0.21 %), PAG 10.0.2 (91.38 ± 0.56 % and 1.01 ± 0.24 %), 8/0.1 (91.11 ± 0.39 % and 1.60 ± 0.58 %), and 5/0.05 (89.32 ± 0.97 % and 1.02 ± 0.40 %), indicates that apoptosis did not accompany the decrease in cell proliferation on the soft PAG 5/0.05 matrix (Fig.II.5).

Glass

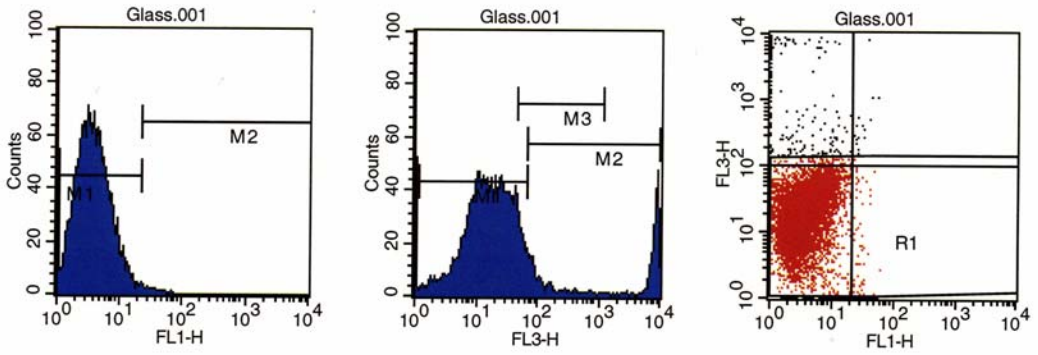

Histogram Statistics

File: Glass.001
Sample ID: Glass
Acquisition Date: 21-Mar-08
Gated Events: 8845
X Parameter: FL1-H (Log)

Log Data Units: Linear Values
Patient ID: Static Ctrl
Gate: G1
Total Events: 10000

Marker	Left, Right	Events	% Gated	% Total	Mean	Geo Mean	CV	Median	Peak Ch
All	1, 9910	8845	100.00	88.45	4.42	3.63	80.51	3.46	1
M1	1, 22	8785	99.32	87.85	4.24	3.57	66.08	3.46	1
M2	22, 9910	63	0.71	0.63	29.56	28.76	25.86	26.66	22

Histogram Statistics

File: Glass.001
Sample ID: Glass
Acquisition Date: 21-Mar-08
Gated Events: 10000
X Parameter: FL3-H (Log)

Log Data Units: Linear Values
Patient ID: Static Ctrl
Gate: No Gate
Total Events: 10000

Marker	Left, Right	Events	% Gated	% Total	Mean	Geo Mean	CV	Median	Peak Ch
All	1, 9910	10000	100.00	100.00	660.06	27.92	315.89	19.11	1
M1	1, 69	8519	85.19	85.19	20.90	15.81	71.79	16.40	10
M2	69, 9910	1312	13.12	13.12	4895.53	1769.62	72.20	6915.82	8058
M3	47, 1197	1102	11.02	11.02	95.61	75.63	117.75	63.21	48

Quadrant Statistics

File: Glass.001
Sample ID: Glass
Acquisition Date: 21-Mar-08
Gated Events: 10000
X Parameter: FL1-H (Log)
Quad Location: 21, 100

Log Data Units: Linear Values
Patient ID: Static Ctrl
Gate: No Gate
Total Events: 10000
Y Parameter: FL3-H (Log)

Quad	Events	% Gated	% Total	X Mean	X Geo Mean	Y Mean	Y Geo Mean
UL	1047	10.47	10.47	2.04	1.34	6101.87	3774.90
UR	19	0.19	0.19	31.22	30.15	762.41	336.46
LL	8796	87.96	87.96	4.27	3.59	22.28	16.07
LR	138	1.38	1.38	30.64	29.75	10.95	2.70

Figure II.4.i. Flow cytometric analysis for apoptotic cells seeded on glass. The UL, UR, LL, and LR quadrants represents dead cells, cells in end stage apoptosis, viable cells, and apoptotic cells, respectively. Cells seeded on glass had an average of 91.0 ± 1.1 % viable cells and a small amount of cells in apoptosis averaging 0.89 ± 0.21 %.

PAG 10/0.2

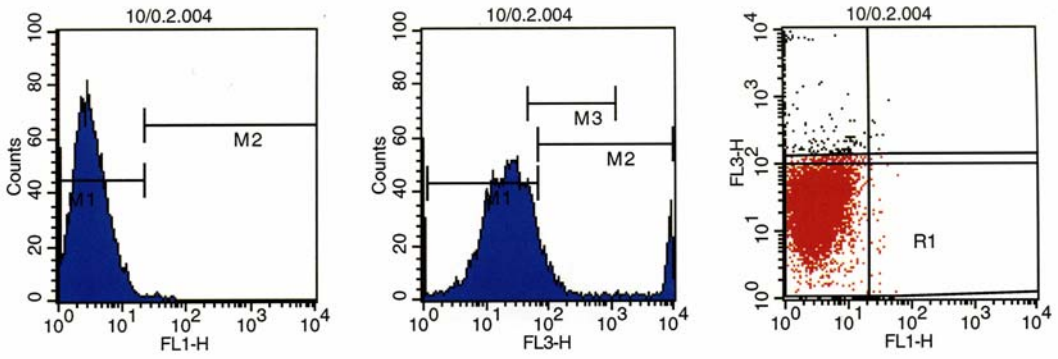

Histogram Statistics

File: 10/0.2.004
Sample ID: 10/0.2
Acquisition Date: 21-Mar-08
Gated Events: 9240
X Parameter: FL1-H (Log)

Log Data Units: Linear Values
Patient ID: Static Ctrl
Gate: G1
Total Events: 10000

Marker	Left, Right	Events	% Gated	% Total	Mean	Geo Mean	CV	Median	Peak Ch
All	1, 9910	9240	100.00	92.40	3.65	3.05	76.26	2.94	1
M1	1, 22	9211	99.69	92.11	3.57	3.03	64.02	2.94	1
M2	22, 9910	29	0.31	0.29	30.72	29.69	29.55	30.51	31

Histogram Statistics

File: 10/0.2.004
Sample ID: 10/0.2
Acquisition Date: 21-Mar-08
Gated Events: 10000
X Parameter: FL3-H (Log)

Log Data Units: Linear Values
Patient ID: Static Ctrl
Gate: No Gate
Total Events: 10000

Marker	Left, Right	Events	% Gated	% Total	Mean	Geo Mean	CV	Median	Peak Ch
All	1, 9910	10000	100.00	100.00	424.35	30.58	393.44	24.36	1
M1	1, 69	8643	86.43	86.43	24.99	20.01	62.84	21.10	31
M2	69, 9910	1304	13.04	13.04	3089.21	608.29	117.68	156.79	8058
M3	47, 1197	1754	17.54	17.54	87.76	74.34	101.33	64.36	50

Quadrant Statistics

File: 10/0.2.004
Sample ID: 10/0.2
Acquisition Date: 21-Mar-08
Gated Events: 10000
X Parameter: FL1-H (Log)
Quad Location: 21, 100

Log Data Units: Linear Values
Patient ID: Static Ctrl
Gate: No Gate
Total Events: 10000
Y Parameter: FL3-H (Log)

Quad	Events	% Gated	% Total	X Mean	X Geo Mean	Y Mean	Y Geo Mean
UL	852	8.52	8.52	2.70	1.68	4682.19	1749.82
UR	11	0.11	0.11	28.86	28.18	297.76	251.31
LL	9079	90.79	90.79	3.55	3.02	27.58	21.18
LR	58	0.58	0.58	30.57	29.47	11.31	2.98

Figure II.4.ii. Flow cytometric analysis for apoptotic cells seeded on PAG 10/0.2. Cells seeded on PAG 10/0.2 had a high percentage of viable cells averaging 91.38 ± 0.56 % and a low percentage of apoptotic cells at 1.01 ± 0.24 %. The percentages are similar to those of cells seeded on glass.

PAG 8/0.1

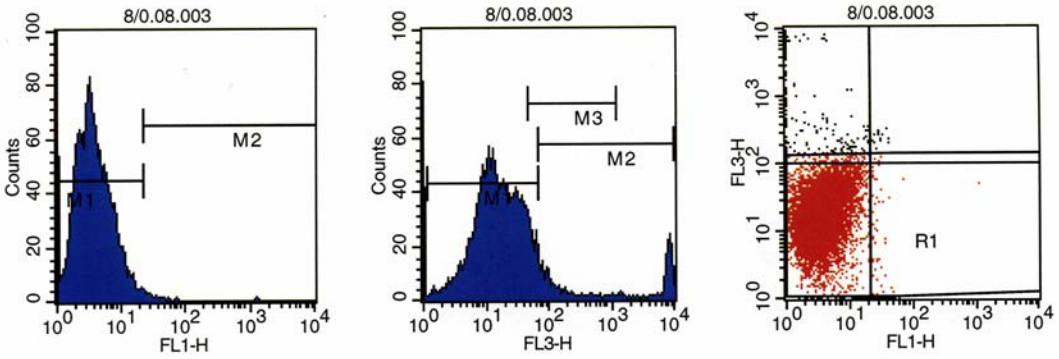

Histogram Statistics

File: 8/0.08.003
Sample ID: 8/0.08
Acquisition Date: 21-Mar-08
Gated Events: 9275
X Parameter: FL1-H (Log)

Log Data Units: Linear Values
Patient ID: Static Ctrl
Gate: G1
Total Events: 10000

Marker	Left, Right	Events	% Gated	% Total	Mean	Geo Mean	CV	Median	Peak Ch
All	1, 9910	9275	100.00	92.75	4.54	3.65	275.81	3.46	1
M1	1, 22	9226	99.47	92.26	4.29	3.61	65.86	3.46	1
M2	22, 9910	51	0.55	0.51	50.98	29.95	312.59	26.42	22

Histogram Statistics

File: 8/0.08.003
Sample ID: 8/0.08
Acquisition Date: 21-Mar-08
Gated Events: 10000
X Parameter: FL3-H (Log)

Log Data Units: Linear Values
Patient ID: Static Ctrl
Gate: No Gate
Total Events: 10000

Marker	Left, Right	Events	% Gated	% Total	Mean	Geo Mean	CV	Median	Peak Ch
All	1, 9910	10000	100.00	100.00	387.20	22.12	408.91	16.70	1
M1	1, 69	8945	89.45	89.45	19.80	15.09	72.98	14.86	10
M2	69, 9910	966	9.66	9.66	3825.04	1028.36	93.81	5327.98	7431
M3	47, 1197	1048	10.48	10.48	99.59	77.99	117.83	64.07	60

Quadrant Statistics

File: 8/0.08.003
Sample ID: 8/0.08
Acquisition Date: 21-Mar-08
Gated Events: 10000
X Parameter: FL1-H (Log)
Quad Location: 21, 100

Log Data Units: Linear Values
Patient ID: Static Ctrl
Gate: No Gate
Total Events: 10000
Y Parameter: FL3-H (Log)

Quad	Events	% Gated	% Total	X Mean	X Geo Mean	Y Mean	Y Geo Mean
UL	708	7.08	7.08	2.61	1.54	5185.91	2535.90
UR	18	0.18	0.18	30.09	29.56	209.38	197.90
LL	9177	91.77	91.77	4.27	3.61	21.30	15.60
LR	97	0.97	0.97	42.28	30.61	10.83	3.01

Figure II.4.iii. Flow cytometric analysis for apoptotic cells seeded on PAG 8/0.1. Cells seeded on PAG 8/0.1 also had a high percentage of cell viability (about 91.11 ± 0.39 %) similar to those on glass and PAG 10/0.2. The percentage of apoptotic cells was low averaging 1.60 ± 0.58 %.

PAG 5/0.05

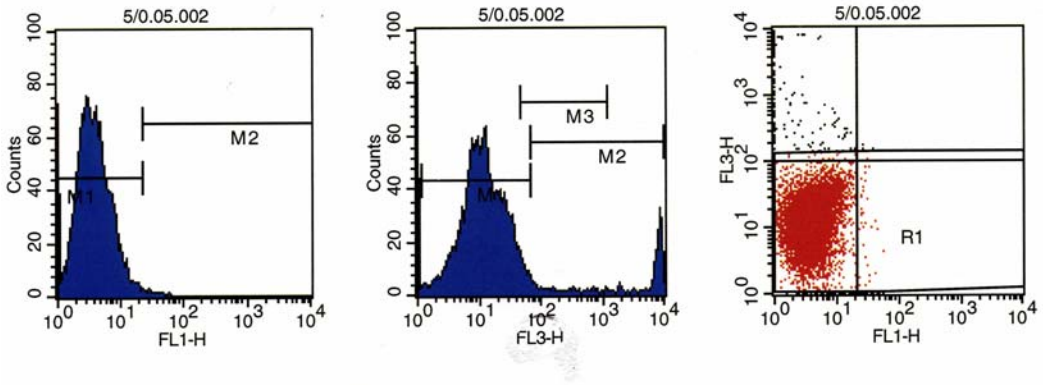

Histogram Statistics

File: 5/0.05.002
Sample ID: 5/0.05
Acquisition Date: 21-Mar-08
Gated Events: 9120
X Parameter: FL1-H (Log)

Log Data Units: Linear Values
Patient ID: Static Ctrl
Gate: G1
Total Events: 10000

Marker	Left, Right	Events	% Gated	% Total	Mean	Geo Mean	CV	Median	Peak Ch
All	1, 9910	9120	100.00	91.20	4.29	3.63	71.81	3.43	2
M1	1, 22	9086	99.63	90.86	4.20	3.60	62.74	3.43	2
M2	22, 9910	34	0.37	0.34	29.64	28.95	24.16	27.76	25

Histogram Statistics

File: 5/0.05.002
Sample ID: 5/0.05
Acquisition Date: 21-Mar-08
Gated Events: 10000
X Parameter: FL3-H (Log)

Log Data Units: Linear Values
Patient ID: Static Ctrl
Gate: No Gate
Total Events: 10000

Marker	Left, Right	Events	% Gated	% Total	Mean	Geo Mean	CV	Median	Peak Ch
All	1, 9910	10000	100.00	100.00	503.11	18.51	360.62	12.19	1
M1	1, 69	9032	90.32	90.32	15.15	11.67	76.13	11.34	12
M2	69, 9910	868	8.68	8.68	5638.71	3194.69	53.34	7169.17	7169
M3	47, 1197	401	4.01	4.01	149.58	93.98	136.13	65.52	52

Quadrant Statistics

File: 5/0.05.002
Sample ID: 5/0.05
Acquisition Date: 21-Mar-08
Gated Events: 10000
X Parameter: FL1-H (Log)
Quad Location: 21, 100

Log Data Units: Linear Values
Patient ID: Static Ctrl
Gate: No Gate
Total Events: 10000
Y Parameter: FL3-H (Log)

Quad	Events	% Gated	% Total	X Mean	X Geo Mean	Y Mean	Y Geo Mean
UL	799	7.99	7.99	1.56	1.17	6118.35	4378.59
UR	4	0.04	0.04	30.42	30.10	145.62	142.98
LL	9132	91.32	91.32	4.23	3.62	15.47	11.60
LR	65	0.65	0.65	29.66	28.82	11.12	3.54

Figure II.4.iv. Flow cytometric analysis for apoptotic cells seeded on PAG 5/0.05. Consistent with the other three harder substrates, PAG 5/0.05 had a high percentage of viable cells averaging 89.32 ± 0.97 % and a low population of apoptotic cells at about 1.02 ± 0.40 %.

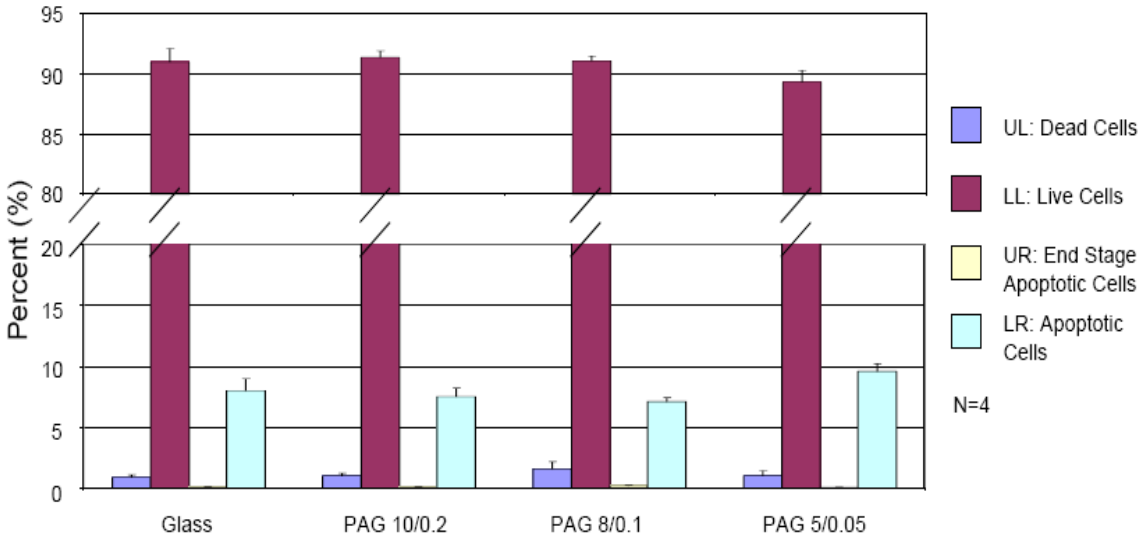

Figure II.5. Quantitative flow cytometric analysis of EC apoptosis. The blue bars represent cells located in the UL quadrant and identifies dead cells in the population. The maroon bars represent cells located in the LL quadrant and identifies viable cells. The ivory bars represent the UR quadrant and identifies cells in end stage apoptosis. The pastel blue bars represent the LR quadrant and identifies cells that are apoptotic. ECs seeded on all four substrates demonstrated similar high percentages of cell viability and low percentages of apoptosis. Error bars represent SEM.

II.D.3. Matrix Rigidity Does Not Affect Cell Elongation or Ellipticity Ratio

Sections II.D.1. and II.D.2. showed that softer matrices decrease EC proliferation, but had little effect on cell apoptosis. For a further understanding of the effects of matrix rigidity, EC morphology was examined. Fig. II.6 shows greater lengths of the long and short axes of cells seeded on glass and PAG 10/0.2 (Fig. II.6.i-ii) and shorter lengths on PAG 8/0.1 and PAG 5/0.05 (Fig. II.6.iii-iv) seeded cells. Using the Metamorph software, the long axis (length) and short axis (width) of the cells were measured (section II.C.7) and compared. In Fig. II.7, the lengths of BAECs seeded on glass and PAG 10/0.2 (90.5 ± 4.1 μm and 90.6 ± 2.6 μm, respectively) are longer than those of cells seeded on PAG 8/0.1 (73.7 ± 1.5 μm) and PAG 5/0.05 (69.6 ± 1.4 μm). A similar trend is seen on the short axis where the cell widths on glass and PAG 10/0.2 are greater at 50.1 ± 3.6 μm and 50.5 ± 2.0 μm, respectively, compared to PAG 8/0.1 at 40.1 ± 0.8 μm and PAG 5/0.05 at 38.3 ± 1.7 μm. The ellipticity ratio was calculated by dividing the long axis by the short axis. Fig. II.8 shows that the average ellipticity ratio for cells seeded on glass, PAG 10/0.2, 8/0.1, and 5/0.05 (1.97 ± 0.09, 1.95 ± 0.07, 1.97 ± 0.02, and 1.94 ± 0.09, respectively) are very similar to each other. This indicates that there were no changes in relative elongation of the cells on the different matrix rigidities.

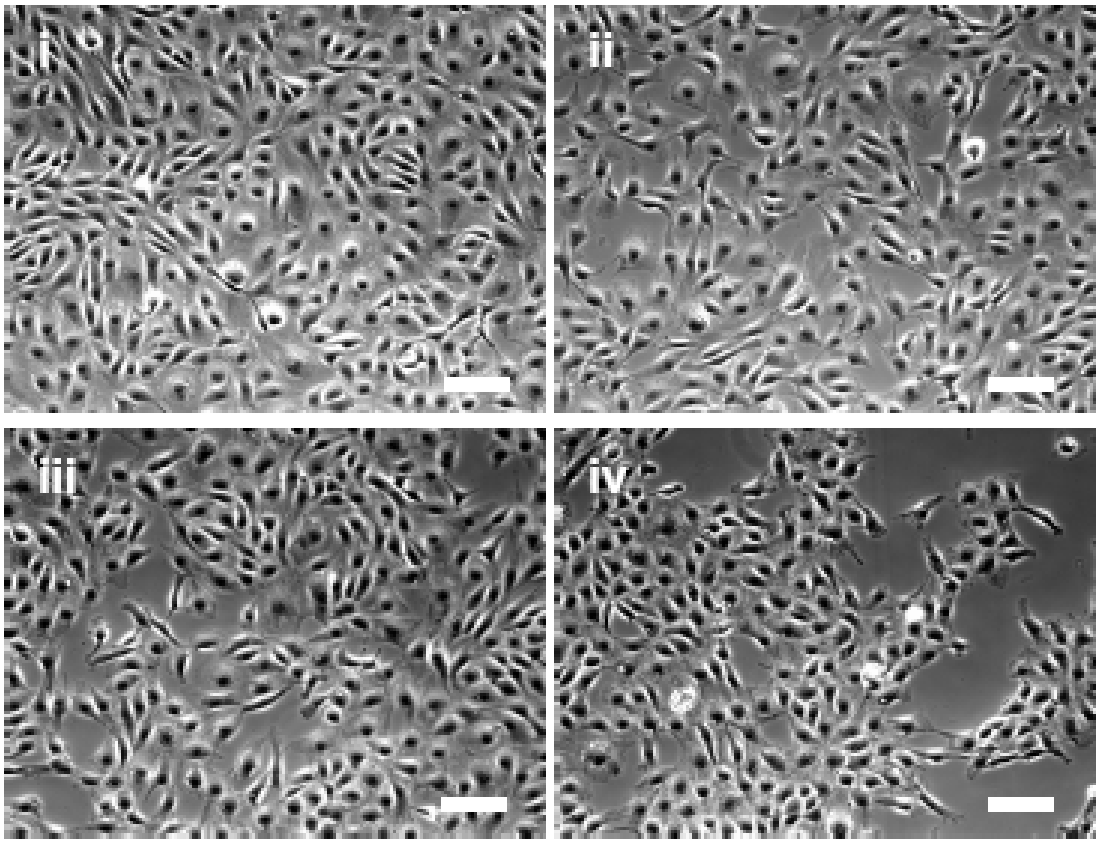

Figure II.6. Phase images of BAEC's seeded on varying substrate rigidities. Phase images of BAECs seeded on (i) Glass, (ii) PAG 10/0.2, (iii) PAG 8/0.1, and (iv) PAG 5/0.05 for 24 hr using a 10x objective. Bar = 100 μm.

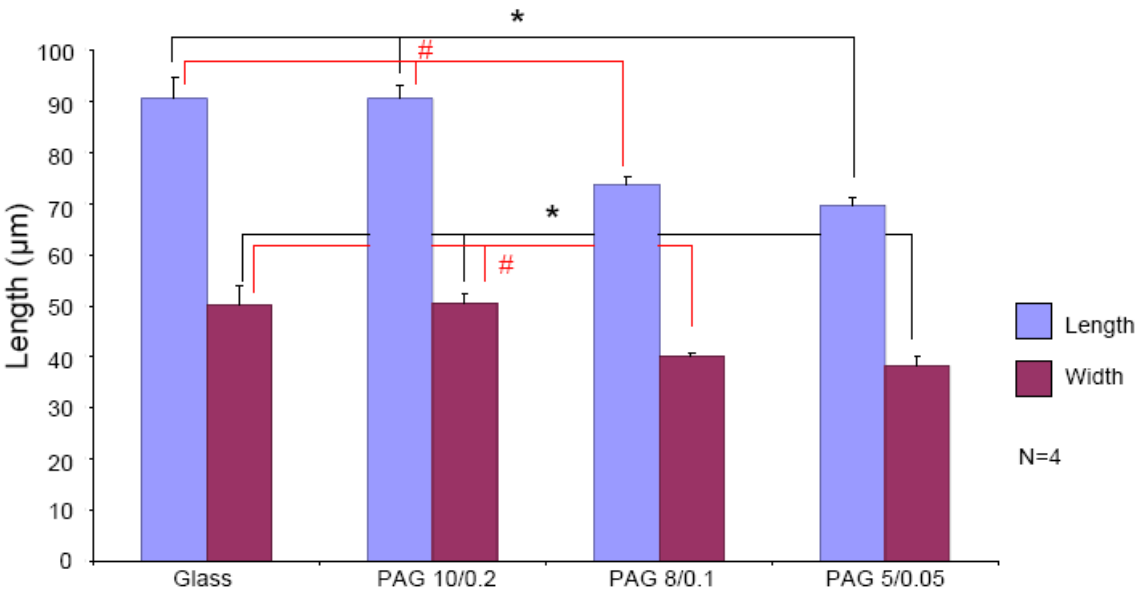

Figure II.7. Quantified long (length) and short (width) axes of BAEC's seeded on substrates with various rigidities. Cells seeded on glass and PAG 10/0.2 have significantly greater length and width than cells seeded on PAG 8/0.1 and PAG 5/0.005. * $P < 0.05$ when compared to PAG 5/0.05. # $P < 0.05$ when compared to PAG 8/0.1. Error bars represent SEM.

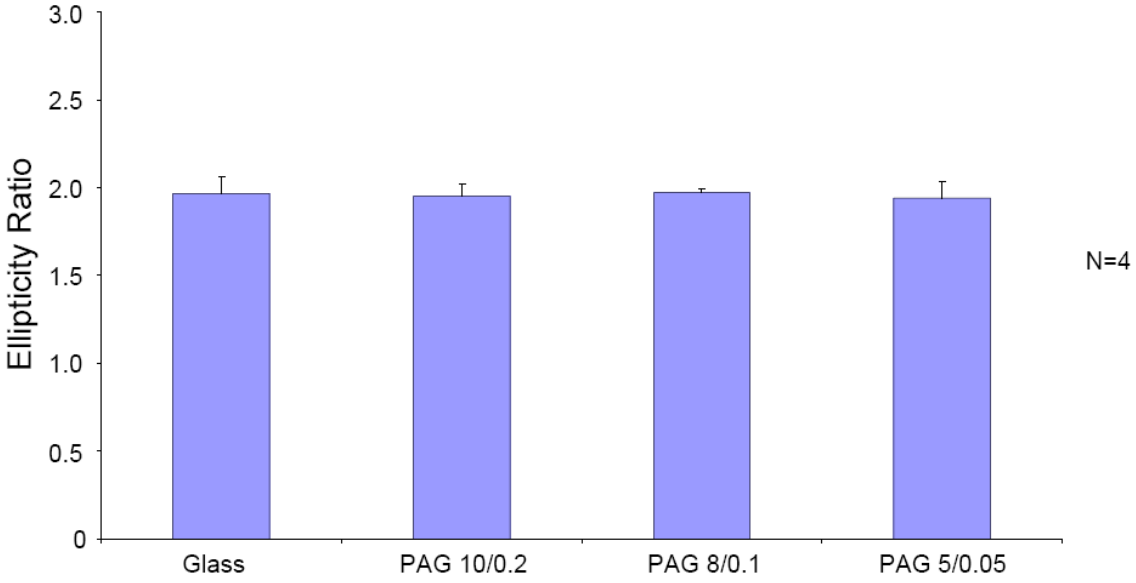

Figure II.8. Ellipticity ratio of cells seeded on various matrix rigidities. The long and short axes of the cells were measured on each of the various substrates. The ellipticity ratio was calculated by dividing the long axis by the short axis. Overall, the ellipticity ratio between the groups was very similar and shows no statistical differences. Error bars represent SEM and N=4.

II.D.4. Matrix Rigidity Affects Cell Area

In the previous section, quantified measurements demonstrated that there is no change in relative cell elongation. However, the changes in both the X and Y axes of the cell indicate that the cells' spreading areas are different among different matrix rigidities. Janmey's group has examined the projected area of BAECs on varying substrate rigidities and observed an increase in projected cell area with harder substrates [2005]. In the current study, a correlation between the increases of cell spreading area and PAG hardness is also observed (Fig. II.6.i-iv). BAECs seeded on glass (Fig. II.6.i) and PAG 10/0.2 (Fig. II.6.ii) substrates had a larger spreading cell area than BAECs seeded on the medium hardness substrate, PAG 8/0.01 (Fig. II.6.iii); whereas the cells seeded on the softest substrate, PAG 5/0.05 (Fig. II.6.iv), had the smallest cell spreading area. The cell spreading area was quantified using the methods outlined in Section II.C.9. Figure II.9 shows that BAECs seeded on glass and PAG 10/0.02 had similar cell spreading areas at $1996 \pm 70.5\ \mu m^2$ and $1897 \pm 89.2\ \mu m^2$, respectively. Cell spreading area decreases on the medium stiffness PAG 8/0.1 ($1554 \pm 121.1\ \mu m^2$) and was smallest on the soft PAG 5/0.05 ($1018 \pm 112.1\ \mu m^2$). Thus, the BAECs seeded on the softer matrix are more compact than those seeded on glass or the hard PAG 10/0.2 matrix. There is no appreciable difference in cell counts between the substrates (Fig. II.10).

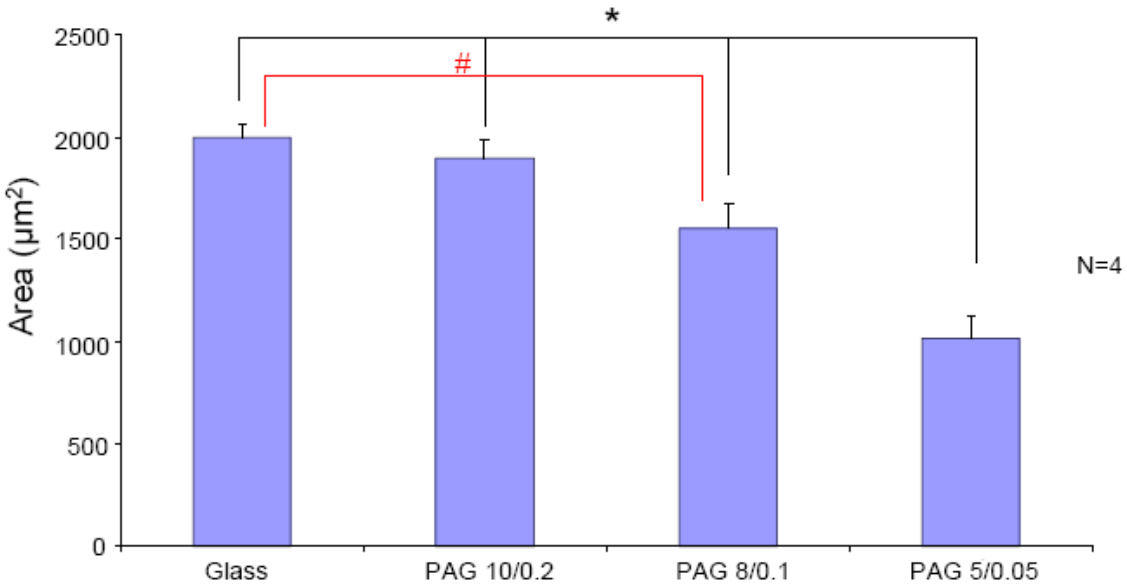

Figure II.9. Quantified cell area analysis. Cell area was quantified using the Image J software. Each bar respresents the mean from four different experiments. * $P < 0.05$ when compared to PAG 5/0.05. # $P < 0.05$ when compared to glass. Error bars represent SEM.

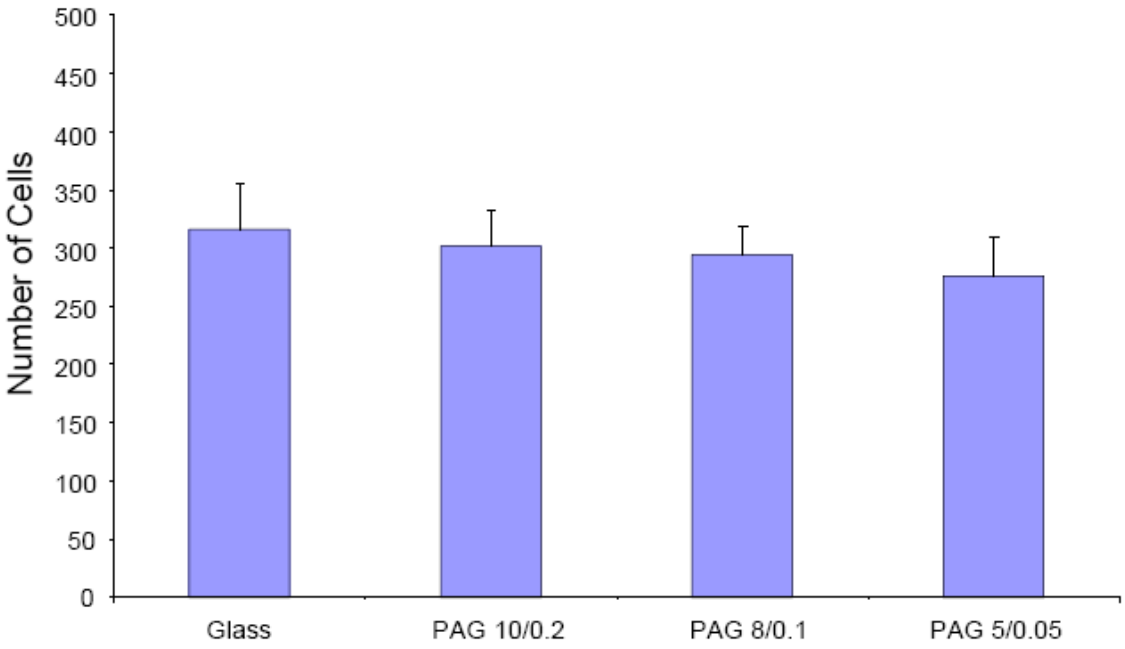

Figure II.10. Cell counts in fields of view of phase images. BAECs seeded onto the various substrates showed a slight decreasing trend in cell count towards softer substrates, but there is no statistically significant difference among the cell counts for different matrices.

II.E. Discussion

In order to establish the relationship between ECM mechanics and EC behavior, the effects of matrix rigidity on EC proliferation and morphology were investigated. A significant finding of this study is that matrix rigidity affects EC proliferation. It is shown for the first time that harder substrate increases EC proliferation, while softer substrate significantly reduces EC proliferation. The decrease in EC proliferation on the softer matrix is not accompanied by cell death or apoptosis. These findings indicate that the matrix rigidity is a contributing factor on EC function, especially in proliferation.

An increase in matrix rigidity causes not only an increase in EC proliferation, but also EC spreading areas. Although ECs seeded on hard substrates of glass and PAG 10/0.2 have greater lengths of the long and short axes of the cell than those seeded on softer matrices, the ellipticity ratio for the four groups were very similar to each other and indicate that the cells were uniform in shape, though different in spreading area. With the increases in the long and short axes of the cell on the harder substrates, there was also a corresponding increase in cell area. ECs on glass and PAG 10/0.2 substrates were spread out versus the much more compact nature of the cells seeded on the soft PAG 5/0.05. Yeung et. al., working on NIH 3T3 fibroblasts and BAECs, also demonstrated an increase in projected cell area when cultured on harder substrates and a decrease on softer substrates [2005]. EC compaction on the softer substrate may indicate that the cells are reorganizing to form tissue structures similar to that in fibroblasts [Guo et. al., 2006] or capillary networks that have been observed in ECs [Vernon et. al., 1992; Vailhe et. al., 1997; Sieminski et. al., 2004]. The spreading of cell area on hard matrix may increase intracellular tension to modulate EC function such as proliferation.

There are studies that show a relationship between cell shape and function. Initial reports of this relationship were done by Folkman et. al. where they regulated cell spreading, controlling cell shape, and found that DNA synthesis and growth to be tightly coupled to this control of cell shape [1978]. Subsequent studies show that varying the fibronectin molecular coating density alters integrin receptor densities and the associated cell spreading and intracellular integrin signaling activities [Ingber et al., 1990; Schwartz et al., 1991; McNamee et al., 1996]. Chen et. al. found that human and bovine capillary ECs switch from growth to apoptotic phases solely based on cell area, regardless of the type of matrix protein or integrin used for adhesion [1997]. Cells use integrin receptors to adhere to the ECM and this binding can activate intracellular signaling cascades and mediate tension-dependent changes in cell cytoskeleton and shape. Huang et. al. demonstrated that the mere induction of integrin signaling by a combination of early basic fibroblast growth factor (bFGF), epidermal growth factor (EGF) and fibronectin are not sufficient for cell growth, but changes in tension-dependent cell area and actin cytoskeletal structure regulates the G_1/S-phase transition for cell proliferation [1998]. The results presented in the current study are in concert with those previous findings, and clearly identify the ECM mechanics as a regulator of cell spreading and subsequent cell behavior.

The results reported here provide a foundation to study EC behaviors in response to its ECM environment. In the next chapter, further studies are performed to examine the signaling pathways that associate substrate rigidity to the changes in EC proliferation.

Chapter III

Roles of Integrins, Src, and Akt in the Regulation of EC Proliferation by Matrix Rigidity

III.A. Abstract

In Chapter II, I have demonstrated that EC proliferation is matrix rigidity dependent. In order to understand the mechanism for this process, I investigated the signaling pathways that transduce signals from the ECM into ECs to regulate proliferation. Through the application of RGD, an integrin blocking peptide, I identified integrins as the early signal transducers to modulate proliferation. Blocking integrins significantly decreased the high level of proliferation of ECs seeded on the hard matrix. The proliferation rates of ECs on different matrix rigidities were reversely correlated with Src and Akt phosphorylation: the harder the matrix, the lower the Src/Akt phosphorylation, and the higher the EC proliferation. The decrease in proliferation of ECs on the hard matrix following RGD treatment was also associated with increases in Src and Akt phosphorylation. Additionally, transfecting ECs with c-$Src_{(WT)}$ cDNA or a constitutively active Akt construct caused increases of Src/Akt phosphorylation accompanied by the decrease of EC proliferation on the hard PAG matrix. Thus, these results confirm the roles of Src and Akt in regulating the matrix rigidity-modulated EC proliferation. The findings of our studies identified the potential molecular mechanisms by which matrix rigidity governs EC proliferation.

III.B. Introduction

There has been an emergence of new data suggesting that changes in the mechanical properties of cellular microenvironment can modulate cell behavior and function. Most cells rely on their anchorage to a solid surface to maintain their viability. It has been shown that cells can sense their surroundings and transmit forces to their surrounding substrate through their myosin-based contractility and cellular adhesions [Ingber, 2002]. Cells can respond to the changes to their surroundings by reorganizing their cytoskeleton, adjusting the contractile forces it exerts on the substrate, and modifying their functional behavior [Discher et al., 2005]. Examination of different cell types on various matrices has shown a correlation between matrix rigidity and cell morphogenesis, homeostatic functions, and disease processes.

With the recent development in science and technology for the investigations of ECM mechanics and cell functions, there are increasing interests in studying the interaction of ECs with ECM. It has been shown that EC capillary networks form on soft gels and not hard gels [Vernon et. al., 1992; Vailhe et. al., 1997; Sieminski et. al., 2004], whereas hard gels increase the projected EC area and circumference [Yueng et. al., 2005]. These observations indicate that the ECM plays a pivotal role in regulating EC function. However, there is a need for more in-depth understanding of how ECs interact with the ECM.

In order to elucidate the molecular mechanism by which the matrix rigidity regulates EC proliferation, I investigated the role of integrin receptors, which translate signals between the ECM and the cells [Boudreau et al., 1999]. The heterodimeric integrin molecules are composed of α and β subunits that are transmembrane receptors

with their cytoplasmic domains interacting with the actin cytoskeleton and associated proteins, and their extracellular domains binding to the ECM. Physical deformation of the ECM or tissues translates to changes in the force distribution across the integrin receptors to result in the reorganization of the cytoskeleton and subsequent downstream signaling within the cell [Ingber, 2002]. Many studies have shown that integrins can affect molecules such as Src, FAK, ERK1/2, NF-κB, Akt, and PI-3 kinase in ECs, SMCs, myocytes, and other cells *in vitro*, as well as in organs of living animals [Alenghat et. al., 2002; Chen et. al., 1999; Franchini et. al., 2000; Urbich et. al., 2002; Rice et. al., 2002; Wang et. al., 2006].

Integrins can indirectly or directly activate Src through FAK or RPTPα [Arias-Salgado et. al., 2003; Eide et. al., 1995; von Wichert et. al., 2003]. Src is a member of the non-receptor tyrosine kinase family that contains one SH2 domain, one SH3 domain, a catalytic domain, and a carboxy-terminal regulatory sequence. Src plays a critical role in a variety of cellular processes, including cell adhesion, spreading, migration, differentiation, apoptosis, and cell cycle progression [Thomas and Brugge, 1997]. Ha and colleagues provide evidence that activated Src plays a role in disrupting endothelial cell-cell junctions by activating downstream Akt/eNOS [2008]. Disruption of cell-cell contacts is an early critical step in capillary morphogenesis.

Akt, also known as PKB, is a serine-threonine kinase activated by PI3K and regulates many critical cellular functions such as migration, proliferation, cell survival, and apoptosis [Shiojima and Walsh, 2002; Chen et. al., 2005; Franke et. al., 1997]. In regards to proliferation, it has been found that Akt can regulate the cell cycle and cellular senescence through the activities of p21, E2F, and MDM2 [Shiojima and Walsh, 2002].

In addition to its effects on proliferation, Akt plays a pivotal role in the viability of ECs after their attachment to the ECM. Integrins mediate the cell attachment to the ECM and induce outside-in signaling that regulates growth factor-dependent EC angiogenesis and cell survival that rely on the PI3K-Akt pathway [Giancotti and Ruoslahti, 1999].

In this chapter, I examined a pathway that transduces signals from the ECM and within ECs to regulate cell proliferation. My results indicate that integrins transduce signals from the ECM into the EC to regulate proliferation, that phosphorylation of Src and Akt leads to a decrease in proliferation, and that blocking integrins increases the phosphorylation of Src and Akt to decrease proliferation. These results provide a molecular mechanism by which matrix rigidity affects EC proliferation.

III.C. Materials and Methods

III.C.1. Cell Culture

All experiments were conducted with BAEC cultures prior to passage 7 and kept in the same culture conditions described in Section II.C.1.

III.C.2. Glass Slide Preparation

The glass microscope slides were prepared according to the methods in Section II.C.2.

III.C.3. Polyacrylamide Gel Preparation

Gel solutions were prepared according to the methods in Section II.C.3.

III.C.4. Fibronectin Coating and Cell Seeding

Fibronectin coating and cell seeding were done according to the methods in Section II.C.5.

III.C.5. Biologic and Pharmacologic Reagents

RGD blocking peptide (GRGDNP, Biomol) was reconstituted in sterile MilliQ water and had a working concentration of 75 μM. The peptide was added to ECs after 4 hr of seeding on various substrates for a total of 20 hr of incubation time.

III.C.6. Cell Proliferation Assay

The cell proliferation assay was done according to the flow cytometric BrdU method in Section II.C.6.

III.C.7. SDS Page and Western Blotting

Cells were washed 2x with ice cold PBS and lysed with a lysis buffer containing 25 mM Tris-HCl, 150 mM NaCl, 1% Triton X-100, 1 mM EDTA, 0.05% SDS, 10 ng/μL leupeptin, 1 mM PMSF, 1 mM $NaVO_4$, and 10 ng/μL aprotinin. The collected lysis buffer was centrifuged at 16,000 rpm for 10 min at 4^{o}C, and the supernatant collected for protein analysis. Protein concentrations were determined by Bradford assay using a Hitachi U-2000 spectrophotometer. The denatured proteins were equally loaded (30 μg) and subjected to protein separation by gel electrophoresis with SDS-PAGE. The proteins were transferred from the gel to a nitrocellulose membrane (Bio-Rad, Hercules, CA), blocked with 5% BSA in TBSt, and probed with various primary antibodies. The bound primary antibodies were detected by using an appropriate secondary antibodies conjugated with IgG-horseradish peroxidase and by using the ECL detection system (Amersham Pharmacia Biotech).

III.C.8. Plasmid Transfection

HA-PKBα – T308D.S473D was previously described [Andjelkovic et. al., 1997]. Mutations were made at threonine 308 and serine 473 to aspartic acid to develop a constitutively active Akt ($Akt_{(CA)}$). The c-$Src_{(WT)}$ cDNA encodes the wild-type c-Src

[Jalali et. al., 1998]. The construct or cDNA were transfected into BAECs at 80% confluence using LipofectAmine (Invitrogen, Carlsbad, CA) in 10-cm Petri dishes per manufacturer's instructions. After an incubation of 24 hr, the cells were washed and kept in 10% FBS complete DMEM for another 24 hr before seeding onto the PAG substrates.

III.C.9. Statistical Analysis

One-way ANOVA was used to test the difference between multiple groups, followed by the Dunnett's post hoc test using the JMP7 software (S.A.S Institute Inc., Cary, NC) to determine which groups differ through pair-wise comparisons. If multiple groups were not involved, then data were analyzed by paired Student's t-test. Results were expressed as mean ± SEM from at least 3 independent experiments. Immunoblots were analyzed through densitometry using Image J (NIH) and normalized to the total protein amount for each respective sample. * P values < 0.05 were considered to be statistically significant.

III.D. Results

III.D.1. RGD Blocking Peptide Inhibits Proliferation of ECs Seeded on Hard PAG 10/0.2 Matrix

Integrins are known mechanotransducers that sense physical distortions of the ECM and can affect subsequent downstream signaling within the cell [Ingber, 2002]. In Chapter II, it was demonstrated that the EC proliferation rate was high when seeded on hard matrix, while the rate was low on the soft matrix. I hypothesize that integrins are the initial signal transducers between the ECM and ECs in up-regulating the cell proliferation on hard matrix.

RGD is an integrin blocking peptide that can block a wide range of integrins. The blocking peptide was added to the media after the ECs had been seeded for 4 hr on different matrices and allowed to incubate for 20 hr. To simplify the comparisons, the RGD inhibition experiments were performed only on the hard PAG 10/0.2 matrix and the softest PAG 5/0.05 matrix. After RGD treatment, ECs were collected and analyzed for proliferation using the BrdU incorporation on the flow cytometer as described in Section III.C.6 (Fig. III.1.i). The results of control (untreated) ECs on the hard PAG 10/0.2 matrix showed a higher proliferation rate, as indicated by the high percentage of cells in the S-phase (42.35 ± 1.08 %), than those on the soft PAG 5/0.05 matrix (19.50 ± 1.67 %). Treatment with RGD significantly decreased the proliferation of ECs on the hard PAG 10/0.2 matrix (26.82 ± 3.34 %) with more cells entering into the quiescent G_0-G_1 phase (62.20 ± 3.48 % vs. 38.76 ± 2.85 % in untreated control). Treatment with RGD also caused a small, but statistically significant reduction of the proliferation of ECs on the

soft PAG 5/0.05 matrix (from 19.5±1.67 % for the untreated control to 12.71 ± 1.72 %) (Fig. III.1.ii).

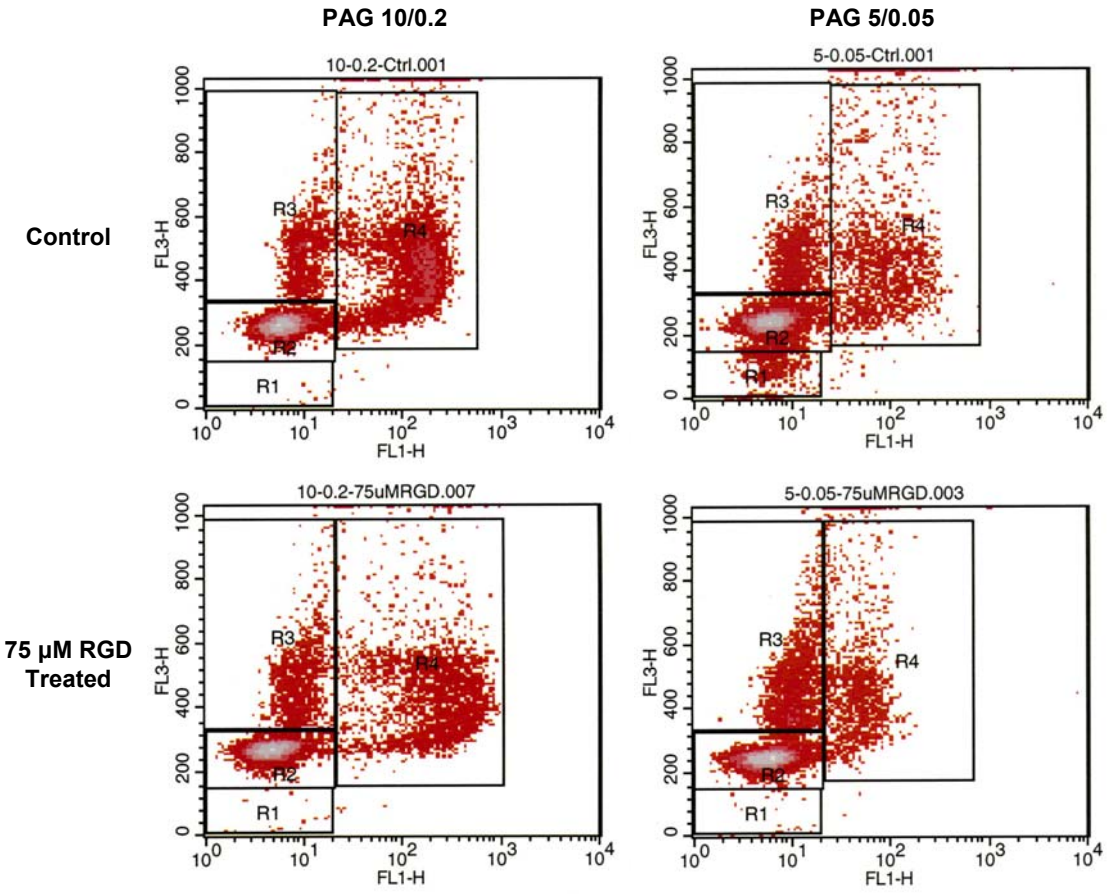

Percent (%) of Cells	**PAG 10/0.2 Control**	**PAG 5/0.05 Control**
Sub G_0-G_1	0.35 ± 0.20	1.43 ± 1.26
G_0-G_1	38.76 ± 2.85	61.27 ± 4.58
G_2 + M phase	16.15 ± 2.77	14.32 ± 3.40
S-phase	42.35 ± 1.08	19.50 ± 1.67 *
	PAG 10/0.2-75µM RGD	**PAG 5/0.05-75µM RGD**
Sub G_0-G_1	0.92 ± 0.51	0.24 ± 0.02
G_0-G_1	62.20 ± 3.48	62.17 ± 10.48
G_2 + M phase	9.41 ± 1.45	22.85 ± 7.80
S-phase	26.82 ± 3.34 #	12.71 ± 1.72 §

Figure III.1.i. Flow cytometric analysis of ECs on hard PAG 10/0.2 and soft PAG 5/0.05 before and after RGD treatment. The cell count "region gate" analysis showed that RGD-treatment significantly decreased the S-phase % of ECs (compared to the respective untreated controls) on the hard PAG 10/0.2 and soft PAG 5/0.05. * $P < 0.05$ compared to PAG 10/0.2 control. # $P < 0.05$ when compared to PAG 10/0.2 control. § $P < 0.05$ when compared to PAG 5/0.05 control

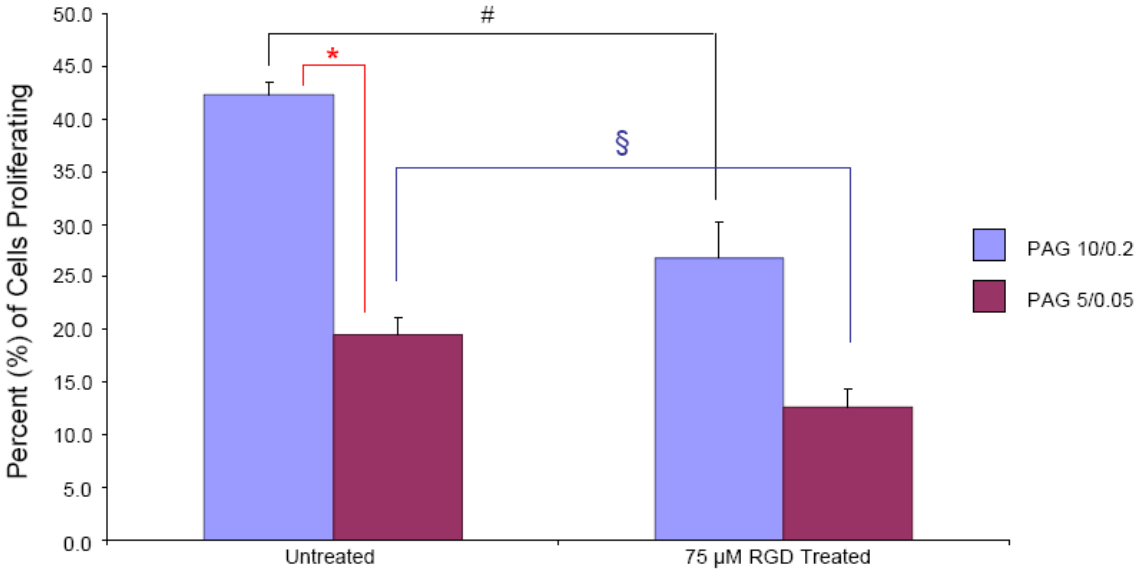

Figure III.1.ii. Flow cytometric analysis of ECs in S-phase after RGD treatment. ECs were treated with 75 µM of RGD after seeding on hard PAG 10/0.2 or soft PAG 5/0.05 matrix. Untreated ECs on PAG 10/0.2 had a significantly higher rate of proliferation vs. those on PAG 5/0.05 (# $P < 0.05$). After RGD treatment, ECs on PAG 10/0.2 significantly decreased their proliferation when compared with the untreated control (* $P < 0.05$). RGD treatment also significantly decreased proliferation of ECs on PAG 5/0.05 when compared the untreated control (§ $P < 0.05$). Error bars represent SEM.

III.D.2. Increase in Src Phosphorylation on Soft PAG 5/0.05 Matrix

Following the identification of the role of integrins in transducing matrix rigidity signals into the cell to regulate proliferation, I proceeded to examine the downstream targets that may relay the signals from the integrins to modulate the cell proliferation pathway. Src was examined because it has been shown to regulate many cellular functions, including cell cycle progression [Thomas and Brugge, 1997]. Determination of phospho-Src in ECs on matrices with different rigidities showed that the level of phospho-Src increased with decreasing matrix rigidity (Fig. III.2). The phospho-Src in the ECs on soft PAG 5/0.05 matrix had a 2.3-fold increase vs. ECs on glass, and a 2.1-fold increase over the hard PAG 10/0.2 matrix. This increase in phospho-Src with decreasing matrix rigidity is opposite in trend to the decrease in proliferation with decreasing matrix rigidity (Fig. III.3.i). The correlation between the two sets of data was determined with the equation $R_{X,Y}$ = covariance (X, Y) / (σ_X * σ_Y), where the covariance is the average products of deviation for the two sets of data, and σ is the standard deviation of the data set. Correlating the mean values of proliferation to the mean values of phospho-Src over the range of matrix rigidities studied yielded a correlation coefficient (R) = -0.97 (* $P < 0.05$). This indicates a very high degree of negative linear relationship between Src phosphorylation and proliferation (Fig. III.3.ii).

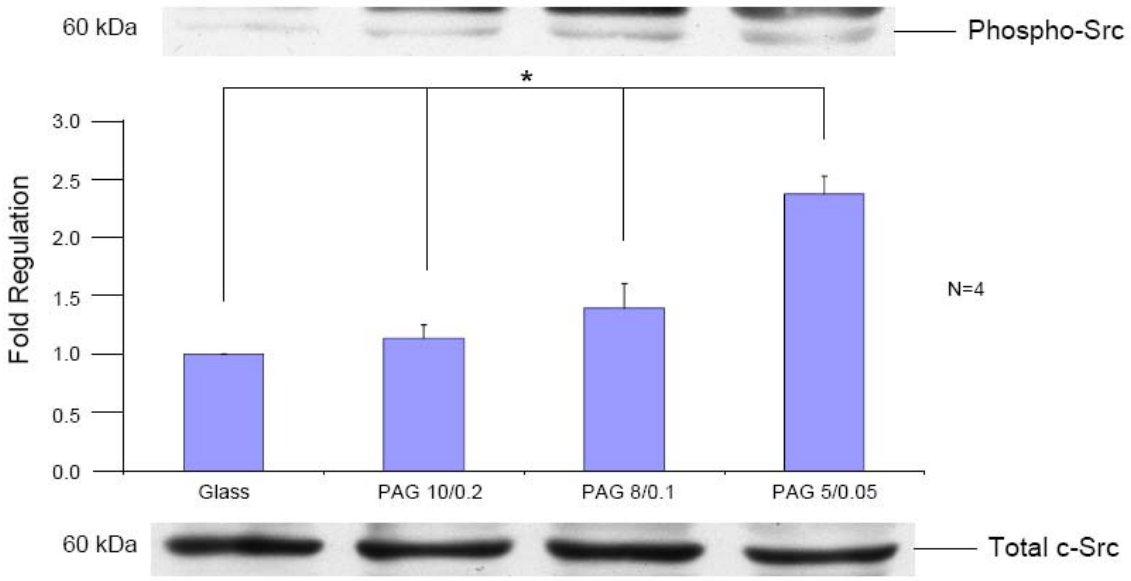

Figure III.2. Phosphorylation of Src on matrices with varying rigidities. ECs were on glass, PAG 10/0.2, PAG 8/0.1, and PAG 5/0.05 substrates, then lysed, and probed for phospho-Src. Phosphorylation of Src increases with decrease matrix rigidity. * $P < 0.05$ when compared to PAG 5/0.05. Error bars represent SEM.

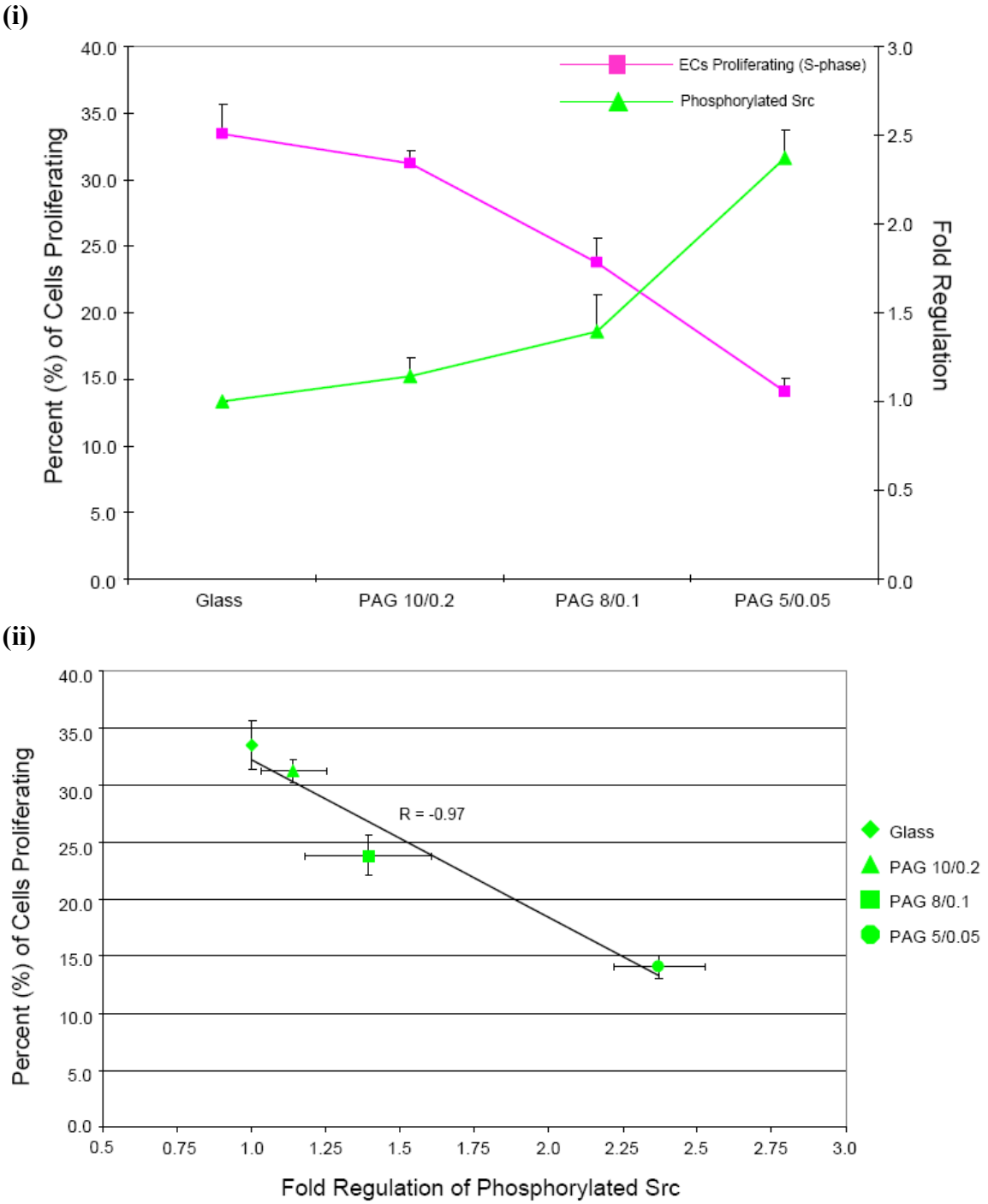

Figure III.3. Correlation of S-phase proliferation and expression of phosphorylated Src for ECs seeded on matrices with various rigidities. (i) The mean values of proliferation (S-phase) and Src phosphorylation on Glass, PAG 10/0.2, PAG 8/0.1 and PAG 5/0.05 substrates. (ii) Plot of the mean values of EC proliferation vs. the fold change of phosphorylated Src for the four matrix conditions. Proliferation and Src phosphorylation show a negative correlation, with a correlation coefficient (R) = -0.97 (* $P < 0.05$). Error bars represent SEM.

III.D.3. Increase in Akt Phosphorylation on Soft PAG 5/0.05 Matrix

Among other possible downstream protein targets of integrins, Akt has been shown to regulate cell cycle and cell survival [Shiojima and Walsh, 2002; Giancotti and Ruoslahti, 1999]. Examination of Akt activation in ECs on matrices with different rigidities showed that Akt phosphorylation increased with decreasing matrix rigidity (Fig. III.4). The phospho-Akt in ECs on soft PAG 5/0.05 matrix had an approximately 2-fold increase in comparison with the ones on glass and the hard PAG 10/0.2 matrix. This increase in phospho-Akt with decreasing matrix rigidity is opposite in trend to the decrease in proliferation with decreasing matrix rigidity (Fig. III.5.i) and is similar to the trend with phospho-Src vs. proliferation (Fig. III.3.i). Correlation of the mean values of phospho-Akt to the mean values of proliferation for ECs on the various matrix rigidities showed a correlation coefficient, R, of -0.96 (* $P < 0.05$)(Fig. III.5.ii). This correlation between phospho-Akt and proliferation is similar to that between phospho-Src and proliferation (Fig. III.3.i). Both molecules have a negative linear relationship with proliferation on the varying matrix rigidities, with a strong negative correlation coefficient.

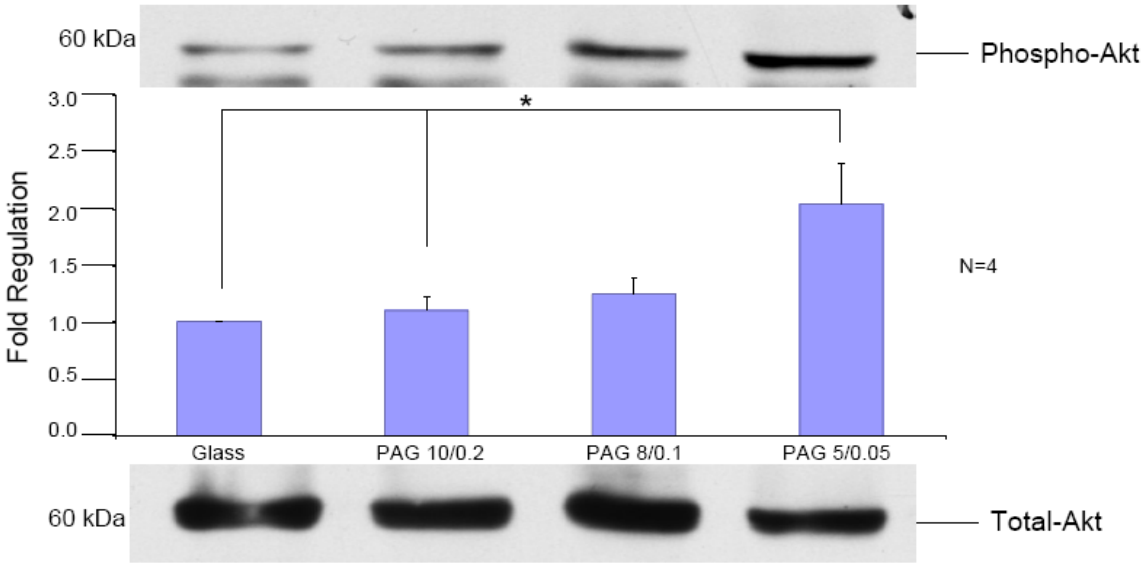

Figure III.4. Phosphorylation of Akt on matrices with various rigidities. ECs were seeded on glass, PAG 10/0.2, PAG 8/0.1, and PAG 5/0.05 substrates, then lysed, and probed for phospho-Akt. Phosphorylation of Akt increases with decrease in matrix rigidity. * $P < 0.05$ when compared to PAG 5/0.05. Error bars represent SEM.

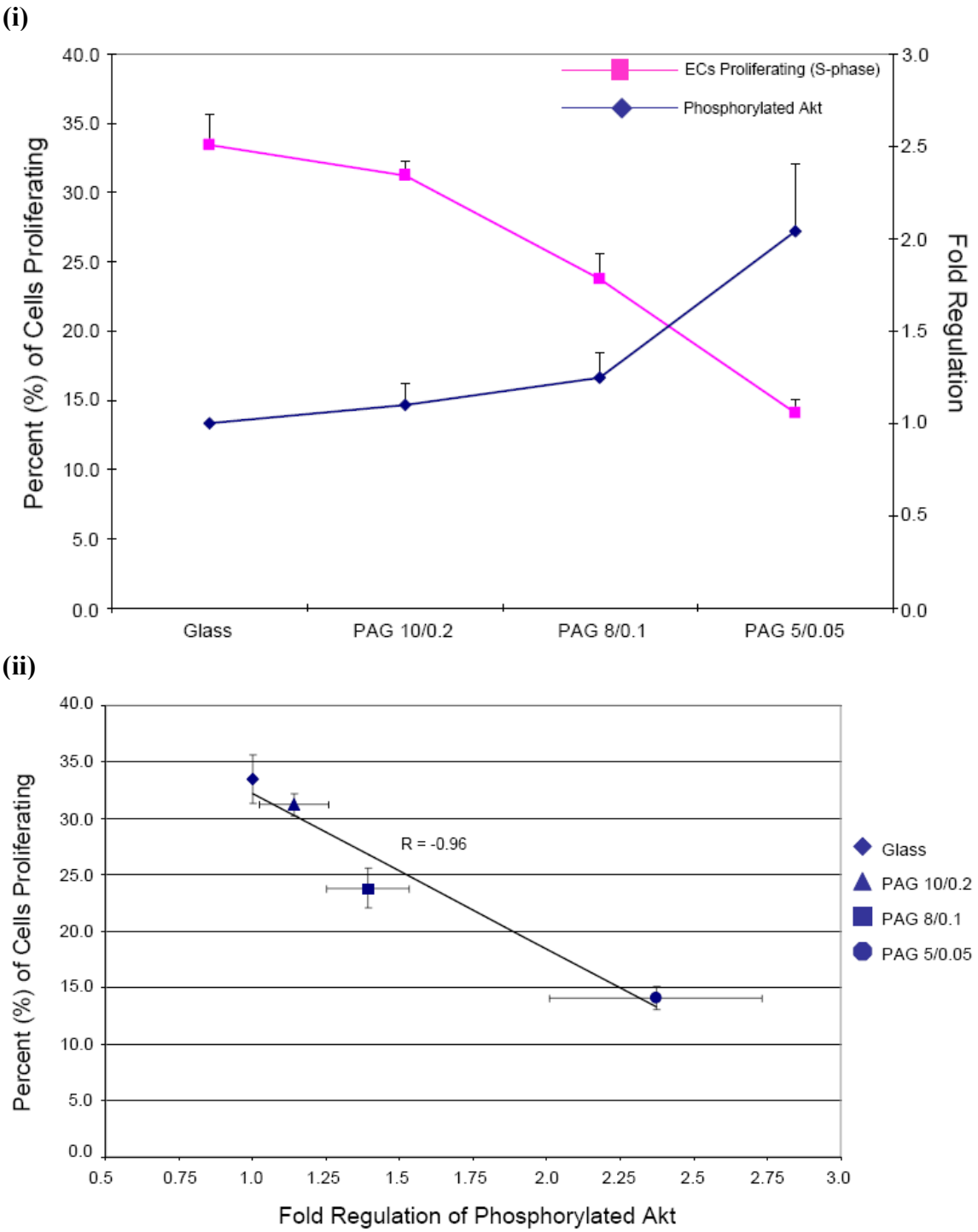

Figure III.5. Correlation of S-phase proliferation with expression of phosphorylated Akt in ECs seeded on various matrix rigidities. (i) Comparison of the mean value data sets of proliferation (S-phase) vs. Akt phosphorylation of ECs seeded on glass, PAG 10/0.2, PAG 8/0.1 and PAG 5/0.05 substrates. (ii) Plot of the mean values of EC proliferation vs. the fold regulation of phosphorylated Akt for ECs on the four substrates. The correlation coefficient (R) = -0.96 (* $P < 0.05$). Error bars represent SEM.

III.D.4. RGD Blocking Peptide Increases Phospho-Src on Hard PAG 10/0.2 Matrix

In Section III.D.1, the RGD integrin blocking peptide was shown to decrease EC proliferation on the hard PAG 10/0.2 substrate, indicating that integrins play an important role in modulating EC proliferation as a function of matrix rigidity. In section III.D.2, Src phosphorylation was identified to be negatively related to the increase in EC proliferation with high matrix rigidity. To determine whether the integrin effect was mediated by modulation of Src activation, the RGD blocking peptide was applied to examine the Src activation in ECs on different matrices. After RGD (75 μM) treatment for 20 hr, the phospho-Src activity of ECs on the hard PAG 10/0.2 matrix was increased to a level similar to that of the untreated ECs seeded on the soft PAG 5/0.05 matrix (Figure III.6). This finding suggests that blocking integrins triggers the activation of Src, which leads to the decrease of EC proliferation (Fig. III.7). RGD had little effect on Src activation in ECs on the soft PAG 5/0.05 matrix.

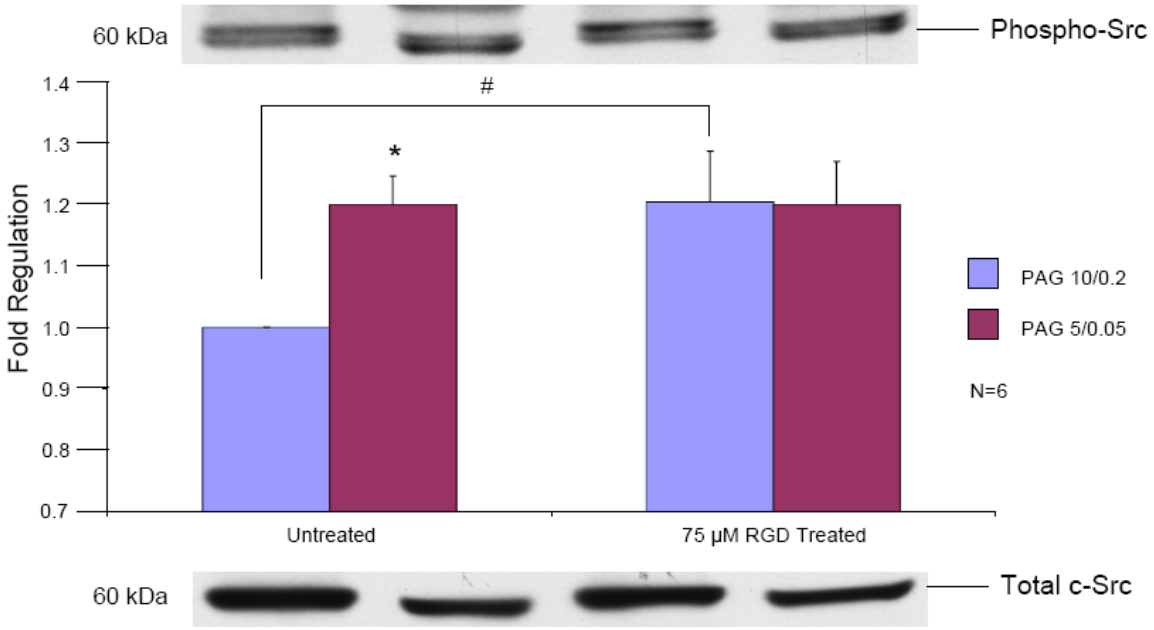

Figure III.6. The effects of RGD treatment on Src phosphorylation in ECs on hard PAG 10/0.2 and soft PAG 5/0.05. ECs on PAG 10/0.2 and PAG 5/0.05 were treated with 75 µM of RGD, lysed, and probed for phospho-Src. RGD-treated ECs on the hard PAG 10/0.02 matrix expressed an increased level of Src phosphorylation similar to the untreated soft PAG 5/0.05. RGD-treated ECs on the soft PAG 5/0.05 had no change in expression levels from the untreated. * $P < 0.05$ when compared to untreated PAG 10/0.2. # $P < 0.05$ when compared to 75 µM RGD-treated PAG 10/0.2. Error bars represent SEM.

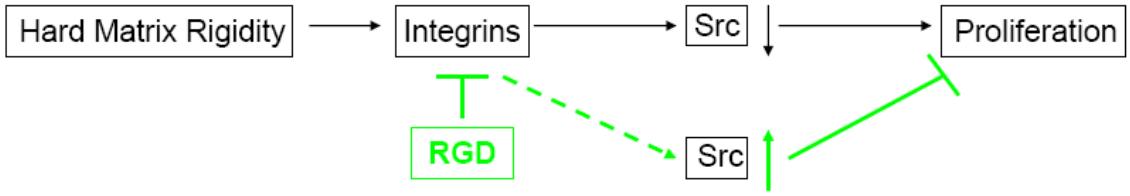

Figure III.7. Schematic flow chart illustration of the effects of RGD on Src phosphorylation and EC proliferation. On the hard matrix substrate, RGD blocks integrins in ECs to increase Src phosphorylation and decrease EC proliferation.

III.D.5. RGD Blocking Peptide Increases Phospho-Akt on Hard PAG 10/0.2 Matrix

In the previous section, applying RGD to ECs seeded on the hard PAG 10/0.2 matrix was shown to increase phospho-Src, while there was no effect on phospho-Src levels in ECs on the soft PAG 5/0.05 matrix. The effect of RGD on phospho-Akt activity was also examined to assess the possible role of integrins in modulating Akt phosphorylation in ECs on various matrices. Using the same methods described in the previous section, we demonstrate that RGD also increased the levels of phospho-Akt in ECs on the hard PAG 10/0.2 matrix to become similar to that in ECs on the soft PAG 5/0.05 (Fig. III.8). Thus, analogous to the case with phospho-Src, blockade of integrins with RGD triggers the activation of phospho-Akt and decrease of EC proliferation (Fig. III.9)

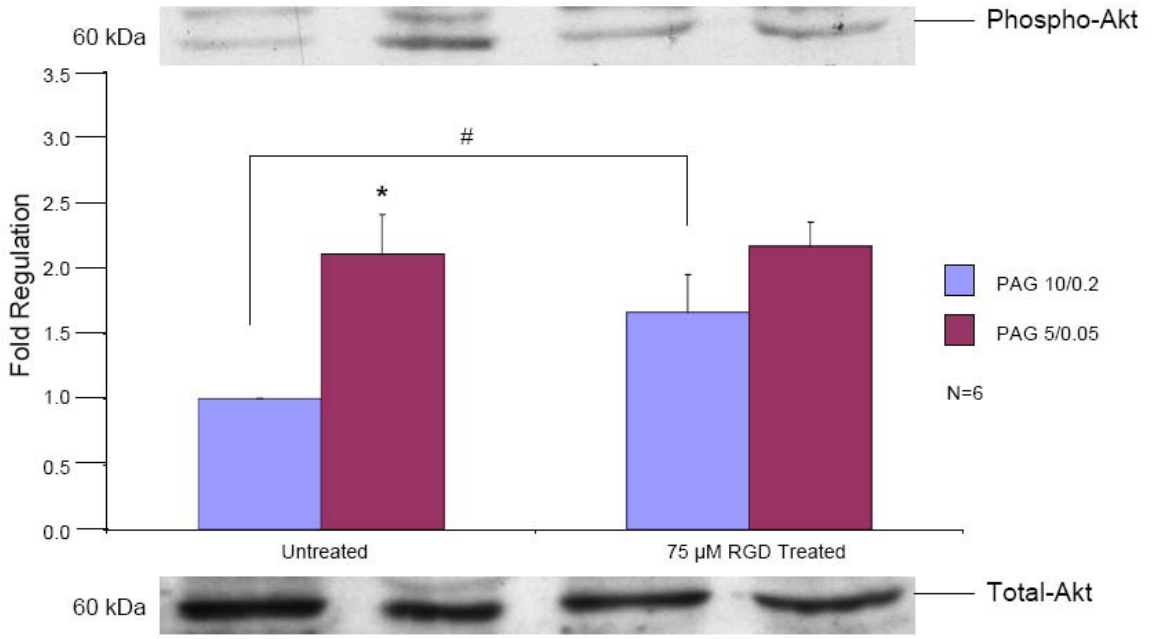

Figure III.8. The effects of RGD on Akt phosphorylation in ECs on hard PAG 10/0.2 and soft PAG 5/0.05. ECs on PAG 10/0.2 and PAG 5/0.05 were treated with 75 µM of RGD, lysed, and probed for phospho-Akt. RGD-treated ECs on the hard PAG 10/0.02 matrix showed a higher level of Akt phosphorylation, which is similar to the untreated soft PAG 5/0.05. RGD-treated ECs on the soft RGD 5/0.05 had no change in phospho-Akt levels from the untreated. * $P < 0.05$ when compared to untreated PAG 10/0.2. # $P < 0.05$ when compared to 75 µM RGD-treated PAG 10/0.2. Error bars represent SEM.

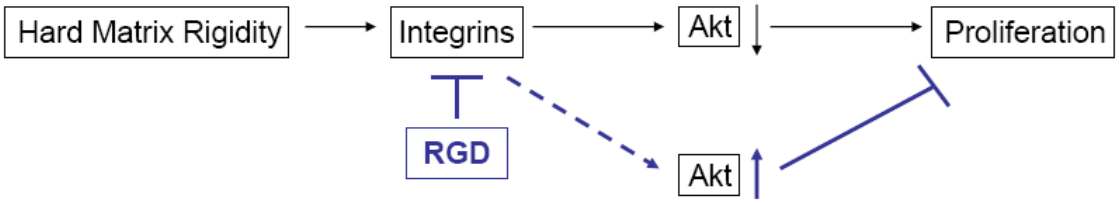

Figure III.9. Schematic flow chart illustration of the effects of RGD on Akt phosphorylation and EC proliferation. On the hard matrix substrate, RGD blocks integrins in ECs to increase Akt phosphorylation and decrease EC proliferation.

III.D.6. Transfection of c-Src$_{(WT)}$ and Constitutively Active Akt Decreases EC Proliferation

Sections III.D.4 and III.D.5 demonstrate the importance of phospho-Src and phospho-Akt in modulating matrix rigidity-regulated EC proliferation. To further ascertain the importance of their roles, ECs were transfected with a c-Src$_{(WT)}$ cDNA or a constitutively active Akt construct (Akt$_{(CA)}$) to determine if they could affect cell proliferation of the ECs seeded on the hard PAG 10/0.2 or soft PAG 5/0.05 matrix. Transfection procedures were done according to the methods outlined in Section III.C.8 with pcDNA used as a vector control, and cells were collected for BrdU incorporation analysis using flow cytometry (Fig. III.10.i). Comparing the different groups of cells in the proliferative S-phase (Fig. III.10.ii), pcDNA-transfected ECs on the hard PAG 10/0.2 matrix showed a proliferation rate of 23.31 ± 0.97 %, which was significantly higher than the pcDNA-transfected ECs on the soft PAG 5/0.05 matrix, 16.08 ± 0.41 %. Src$_{(WT)}$ or Akt$_{(CA)}$-transfected ECs on the hard PAG 10/0.2 matrix both had significantly lower proliferations rates (15.16 ± 1.30 % and 15.01 ± 0.93 %, respectively) in comparison with the pcDNA-transfected ECs on PAG 10/0.2 matrix (23.31 ± 0.97 %), indicating that increases of Src or Akt activities are sufficient in blocking the cell proliferation induced by hard matrix (Fig. III.11.i-ii). It is also of note that the proliferation rates of ECs transfected with the c-Src$_{(WT)}$ or Akt$_{(CA)}$ on the hard matrix had similar proliferation rates to ECs transfected with the same plasmids on the soft matrix. The c-Src$_{(WT)}$-transfected ECs on the soft PAG 5/0.05 matrix had a proliferation rate (11.77 ± 0.32 %) even lower than that of the PAG 5/0.05 pcDNA control (16.08 ± 0.41 %), indicating that an increase in Src activity can further decrease EC proliferation on the soft matrix.

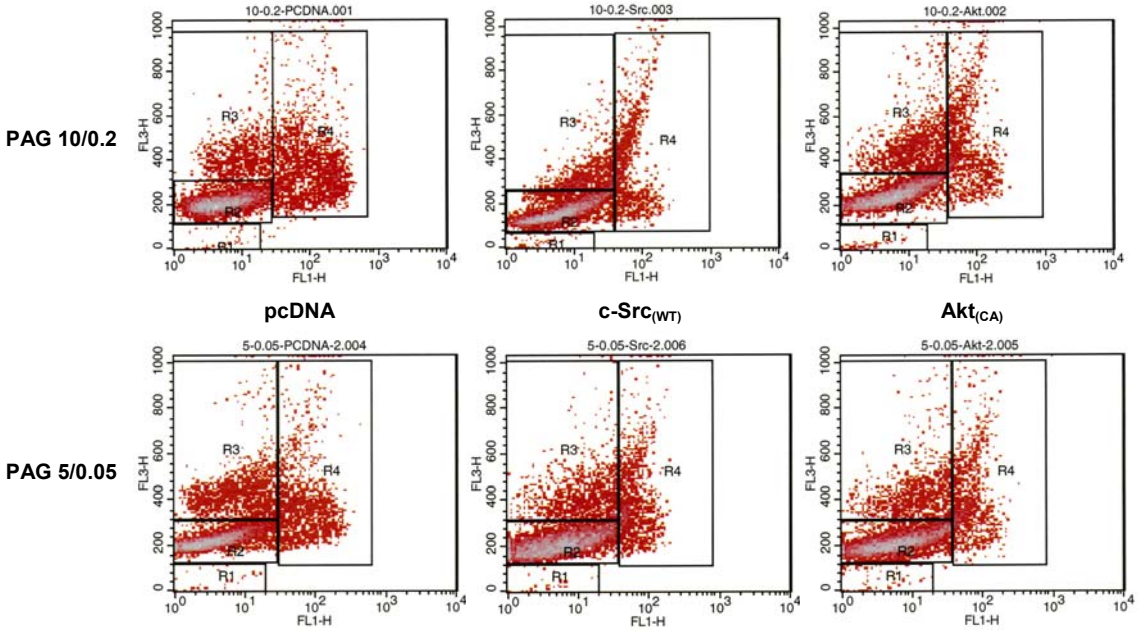

Percent (%) of Cells	**PAG 10/0.2-pcDNA**	**PAG 10/0.2-c-Src$_{(WT)}$**	**PAG 10/0.2-Akt$_{(CA)}$**
Sub G_0-G_1	0.78 ± 0.26	1.17 ± 0.47	1.08 ± 0.08
G_0-G_1	59.59 ± 2.60	66.63 ± 3.04	65.36 ± 0.60
G_2 + M phase	14.96 ± 2.97	15.33 ± 2.17	16.86 ± 0.88
S-phase	23.31 ± 0.97	15.16 ± 1.30 #	15.01 ± 0.93 #
	PAG 5/0.05-pcDNA	**PAG 5/0.05-c-Src$_{(WT)}$**	**PAG 5/0.05-Akt$_{(CA)}$**
Sub G_0-G_1	0.60 ± 0.14	0.49 ± 0.06	0.59 ± 0.07
G_0-G_1	68.44 ± 2.17	72.32 ± 0.84	72.37 ± 1.36
G_2 + M phase	13.78 ± 1.99	14.82 ± 0.79	13.03 ± 0.77
S-phase	16.08 ± 0.41 *	11.77 ± 0.32 §	12.72 ± 0.75

Figure III.10.i. Flow cytometric analysis of ECs seeded on hard PAG 10/0.2 and soft PAG 5/0.05 with the transfection of pcDNA, c-Src$_{(WT)}$, or Akt$_{(CA)}$. The cell count "region gate" analysis showed that transfecting c-Src$_{(WT)}$ or Akt$_{(CA)}$ significantly decreased EC proliferation (S-phase) on hard PAG 10/0.2 matrix compared to the pcDNA-control hard 10/0.2. * $P < 0.05$ when compared to pcDNA-control PAG 10/0.2. # $P < 0.05$ when compared to pcDNA-control PAG 10/0.2. § $P < 0.05$ when compared to pcDNA-control PAG 5/0.05.

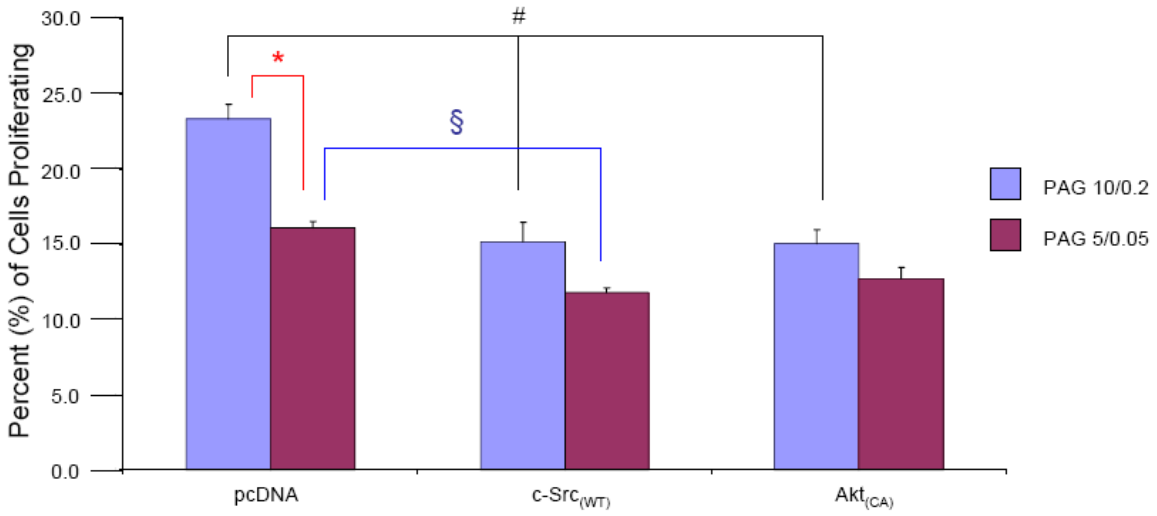

Figure III.10.ii. Flow cytometric analysis of ECs in S-phase with the transfection of pcDNA, c-Src$_{(WT)}$, or constitutively active Akt (Akt$_{(CA)}$). Bar graph comparison of proliferation (S-phase) of ECs transfected with c-Src$_{(WT)}$ or Akt$_{(CA)}$ on PAG 10/0.2 and PAG 5/0.05 matrices. Proliferation rates of the ECs transfected with c-Src$_{(WT)}$ or Akt$_{(CA)}$ had similar levels as the pcDNA-control soft PAG 5/0.05 matrix and the c-Src$_{(WT)}$ or Akt$_{(CA)}$ transfected ECs on the soft matrix. ECs transfected with c-Src$_{(WT)}$ seeded on the soft PAG 5/0.05 matrix did further decrease EC proliferation compared to the pcDNA-control 5/0.05. * $P < 0.05$ when compared to pcDNA-control PAG 10/0.2. # $P < 0.05$ when compared to pcDNA-control PAG 10/0.2. § $P < 0.05$ when compared to pcDNA-control PAG 5/0.05. Error bars represent SEM.

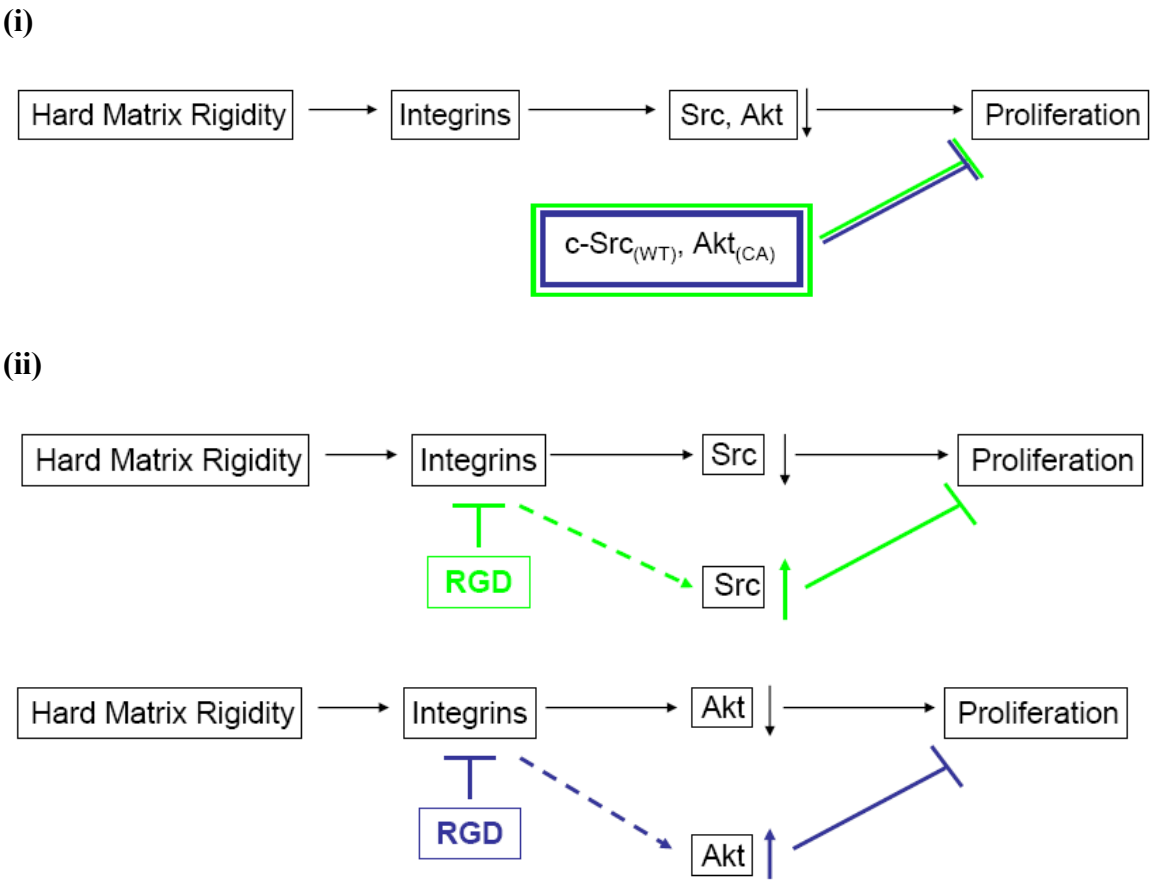

Figure III.11. Schematic flow chart illustration of the effects of Src or Akt on EC proliferation. (i.) Transfecting ECs with c-$Src_{(WT)}$ or $Akt_{(CA)}$ blocks proliferation of ECs seeded on hard matrix rigidity. (ii.) RGD blocking peptide increases Src and Akt phosphorylation and leads to the decrease of EC proliferation on hard matrix.

III.E. Discussion

In this chapter, the signaling pathways that transmit signals from sensing the matrix rigidities to regulate EC proliferation were investigated. Integrins are heterodimeric transmembrane receptors with extracellular domains that bind to the ECM and cytoplasmic domains that associate with the intracellular cytoskeleton. Integrins mediate cell attachment and are known to transduce mechanical stress signals into the cytoskeleton [Ingber, 2002]. The current study demonstrated for the first time that changes in matrix rigidities altered EC proliferation rates. To further investigate this phenomenon, the role of integrins in the signaling process from the ECM to cell proliferation was investigated. Using RGD integrin blocking peptide, it is shown that the inhibition of integrins significantly decreases cell proliferation of ECs on the hard PAG 10/0.2 matrix. Therefore, integrins play an important role in EC attachment to the hard matrix to increase proliferation.

The regulation of matrix rigidity-induced EC proliferation by signaling molecules downstream to integrins was also examined. Various molecules were investigated that are downstream to integrins and have been shown to regulate proliferation and the cell cycle: ERK, p38, p27, β-catenin, and GSK-3β [Pang et al., 2008; Schwartz and Assoian, 2001; Biswas et al., 2006]. None of these molecules showed any significant activity in regulating the matrix rigidity-induced EC proliferation. Src and Akt have also been shown to be the potential integrin downstream molecules that regulate many cellular functions such as migration, apoptosis, and the cell cycle [Thomas and Brugge, 1997; Shiojima and Walsh, 2002; Chen et. al., 2005; Franke et. al., 1997]. In this current study, it is shown that the phosphorylation levels of Src and Akt increase with decreasing matrix

rigidity. The soft PAG 5/0.05 matrix had the highest phosphorylation levels of both Src and Akt, and displayed the lowest proliferation rates. It was shown in Section III.D.1 that RGD treatment decreased the proliferation rate of ECs on the hard PAG 10/0.2 matrix. Therefore, the effects of RGD treatment on Src and Akt phosphorylation were examined. The results showed that the blocking of integrins with RGD increased phospho-Src and phospho-Akt, and these changes were associated with a decrease in EC proliferation. To reinforce the importance of Src and Akt in regulating proliferation, ECs were transfected with c-$Src_{(WT)}$ or $Akt_{(CA)}$ to examine the effects of increased Src and Akt activities on EC proliferation on the varying matrix rigidities. Indeed, similar to RGD-treated ECs on the hard PAG 10/0.02 matrix, the increase in Src or Akt activities led to decreases in EC proliferation rates.

In the current study, the soft PAG 5/0.05 matrix displayed the least amount of EC proliferation that was accompanied by high levels in Src and Akt phosphorylation. Both of these molecules have been shown to regulate cell adhesion and survival. Src phosphorylation was found to be necessary for optimal adhesion to fibronectin and the assembly of actin stress fibers to facilitate cell spreading [Westhoff et al., 2004]. The current study has shown that ECs on soft matrix have a decreased spreading area and high Src phosphorylation. This would indicate that the high Src phosphorylation of ECs on the soft matrix is associated with a low spreading area and hence less cell tension for the induction of cell proliferation. Activation of Akt has also been shown to play a prominent role in maintaining EC viability after cellular attachment [Giancotti and Ruoslahti, 1999]. When cells are subjected to a decrease or absence of cellular attachment, transfection of a constitutively active Akt is able to induce cell survival

[Fujio and Walsh, 1999]. The increase in Akt phosphorylation on the soft matrix with decreased proliferation found in this study corresponds with the work of Fujio and Walsh where they found that Akt activation is necessary for cell survival under conditions that regress angiogenesis [1999].

The results reported here have established the roles of the integrins-Src/Akt pathway in transducing signals from ECM to ECs to mediate the regulation of proliferation by matrix rigidity.

Chapter IV

Summary and Conclusions

Atherosclerosis is a highly prevalent disease that causes the hardening of arteries with plaque formation. Due to the accumulation of lipids, macrophages, other cellular components, and connective tissues within the artery wall, there are many alterations in the physiochemical and geometric features of the cellular microenvironment. These alterations lead to changes in EC function within the vessel. The extracellular matrix (ECM) is a vital component of the cellular microenvironments and has been shown to play an important role in regulating cellular functions such as growth, differentiation, apoptosis, and gene expression [Adams et al., 1993; Boudreau et al., 1999]. Besides the chemical components of ECM, studies of various cell types have shown a correlation between ECM rigidity and cellular functions in health and disease. Observations of the effects of matrix rigidities on cellular behaviors on various cells types, e.g., fibroblasts, myocytes, SMCs, and stem cells, have been made. However, there is a lack of detailed information of EC functions on substrates with different rigidities.

The aims of this dissertation are to investigate the effects of matrix rigidity on EC proliferation and morphology, and elucidate the regulatory mechanisms by which matrix rigidity modulates EC proliferation. Using a synthetic polyacrylamide gel (PAG) substrate and changing the concentrations of acrylamide and bis-acrylamide used in the formulations, gels with various Young's moduli were prepared to mimic softer or harder ECM states for ECs. In Chapter II, I demonstrate that matrix rigidity affects EC proliferation. ECs seeded on hard matrix have significantly higher proliferation rates than the ones on the soft matrix. My study on EC viability on the soft and harder matrices indicates that the decrease in EC proliferation on the soft matrix was not accompanied by any change in apoptosis. EC spreading area increased with increasing matrix rigidity.

The lengths of the long and short axes were longer on ECs seeded on the hard matrix than on the soft matrix, but the ellipticity ratio of the ECs are not significantly different among the various substrates. My results, together with the findings in the literature, suggest that increases in cellular tension induced by cell spreading area and actin cytoskeletal organization can accelerate the cell cycle by transitioning from the G_0-G_1 phase into the S-phase.

In Chapter III, I focused on elucidating the mechanisms underlying the effects of matrix rigidity on EC proliferation. Integrins were chosen for the study as potential candidates for mechanotransduction based on the knowledge that integrins provide a preferred path for transmembrane mechanical force transfer and can induce cellular signal transduction pathways through the cytoskeleton. The application of RGD integrin blocking peptide significantly decreased the proliferation rate of ECs on the hard matrix in comparison to the high proliferation rate in the untreated control state. The RGD also decreased the proliferation rate of ECs on the soft matrix, though to a lesser extent. These results indicate that integrins have a prominent role in mediating matrix-induced EC proliferation. In studying the downstream signaling molecules for the matrix rigidity-regulated proliferation, I found increases in Src and Akt phosphorylation with a decrease in matrix rigidity. Application of RGD blocking peptide to ECs increased the phosphorylation levels of Src and Akt of ECs on hard matrix to levels similar to that expressed in untreated ECs on the soft matrix. These findings indicate that the activation of integrins on hard matrix led to the suppression of Src and Akt activities, with a consequential increase in proliferation. This conclusion was reinforced by the transfection of ECs with a c-$Src_{(WT)}$ cDNA or constitutively active Akt construct before

seeding on the hard or soft matrices. After 24 hr of seeding, BrdU incorporation analysis showed that such enhancement of c-Src or Akt activity significantly reduced the proliferation of ECs seeded on the hard matrix when compared to pcDNA (vector control) transfected ECs seeded on hard matrix. The proliferation rates of the Src/Akt-transfected ECs on the hard matrix were similar to those of the ECs on the soft matrix transfected with pcDNA-control, or the c-$Src_{(WT)}$ or constitutively active Akt. These results show that an increase in Akt or Src activity in ECs through the transfection of c-$Src_{(WT)}$ or constitutively active Akt causes a decline of EC proliferation of cells on the hard matrix. The results of Chapter III indicate that the ECM modulates EC proliferation through the integrin-Src/Akt pathway.

The results of these studies support the hypothesis that matrix rigidity modulates endothelial functions and provide a mechanistic explanation. These findings contribute significantly to the understanding of the endothelial response to their microenvironment, as well as the pathophysiology of atherosclerotic disease in which the arterial wall becomes stiffened.

REFERENCES

Adams JC, Watt FM. 1993. Regulation of development and differentiation by the extracellular matrix. Development (Cambridge, England) 117:1183-98

Ada-Nguema AS, Xenias H, Hofman JM, Wiggins CH, Sheetz MP, Keely PJ. 2006. The small GTPase R-Ras regulates organization of actin and drives membrane protrusions through the activity of PLCepsilon. Journal of cell science 119:1307-19

Alenghat FJ, Ingber DE. 2002. Mechanotransduction: all signals point to cytoskeleton, matrix, and integrins. Sci STKE 2002:PE6

Andjelkovic M, Alessi DR, Meier R, Fernandez A, Lamb NJ, et al. 1997. Role of translocation in the activation and function of protein kinase B. The Journal of biological chemistry 272:31515-24

Arias-Salgado EG, Lizano S, Sarkar S, Brugge JS, Ginsberg MH, Shattil SJ. 2003. Src kinase activation by direct interaction with the integrin beta cytoplasmic domain. Proceedings of the National Academy of Sciences of the United States of America 100:13298-302

Arnett DK, Evans GW, Riley WA. 1994. Arterial stiffness: a new cardiovascular risk factor? American journal of epidemiology 140:669-82

Atabek ME, Kurtoglu S, Pirgon O, Baykara M. 2006. Arterial wall thickening and stiffening in children and adolescents with type 1 diabetes. Diabetes research and clinical practice 74:33-40

Bach TL, Barsigian C, Chalupowicz DG, Busler D, Yaen CH, et al. 1998. VE-Cadherin mediates endothelial cell capillary tube formation in fibrin and collagen gels. Experimental cell research 238:324-34

Baldewsing RA, Mastik F, Schaar JA, Serruys PW, van der Steen AF. 2006. Young's modulus reconstruction of vulnerable atherosclerotic plaque components using deformable curves. Ultrasound in medicine & biology 32:201-10

Balgude AP, Yu X, Szymanski A, Bellamkonda RV. 2001. Agarose gel stiffness determines rate of DRG neurite extension in 3D cultures. Biomaterials 22:1077-84

Beningo KA, Dembo M, Wang YL. 2004. Responses of fibroblasts to anchorage of dorsal extracellular matrix receptors. Proceedings of the National Academy of Sciences of the United States of America 101:18024-9

Biswas P, Canosa S, Schoenfeld D, Schoenfeld J, Li P, et al. 2006. PECAM-1 affects GSK-3beta-mediated beta-catenin phosphorylation and degradation. The American journal of pathology 169:314-24

Boudreau NJ, Jones PL. 1999. Extracellular matrix and integrin signalling: the shape of things to come. The Biochemical journal 339 (Pt 3):481-8

Cary LA, Guan JL. 1999. Focal adhesion kinase in integrin-mediated signaling. Front Biosci 4:D102-13

Chen CS, Mrksich M, Huang S, Whitesides GM, Ingber DE. 1997. Geometric control of cell life and death. Science (New York, N.Y 276:1425-8

Chen J, Somanath PR, Razorenova O, Chen WS, Hay N, et al. 2005. Akt1 regulates pathological angiogenesis, vascular maturation and permeability in vivo. Nature medicine 11:1188-96

Chen KD, Li YS, Kim M, Li S, Yuan S, et al. 1999. Mechanotransduction in response to shear stress. Roles of receptor tyrosine kinases, integrins, and Shc. The Journal of biological chemistry 274:18393-400

Chien S. 2003. Molecular and mechanical bases of focal lipid accumulation in arterial wall. Progress in biophysics and molecular biology 83:131-51

Choquet D, Felsenfeld DP, Sheetz MP. 1997. Extracellular matrix rigidity causes strengthening of integrin-cytoskeleton linkages. Cell 88:39-48

Choy JC, Granville DJ, Hunt DW, McManus BM. 2001. Endothelial cell apoptosis: biochemical characteristics and potential implications for atherosclerosis. Journal of molecular and cellular cardiology 33:1673-90

Crew H. 1919. General Physics: An Elementary Text-book for Colleges. New York: The Macmillan Company

Dai J, Sheetz MP. 1998. Cell membrane mechanics. Methods in cell biology 55:157-71

Danias PG, Tritos NA, Stuber M, Botnar RM, Kissinger KV, Manning WJ. 2003. Comparison of aortic elasticity determined by cardiovascular magnetic resonance imaging in obese versus lean adults. The American journal of cardiology 91:195-9

Danias PG, Tritos NA, Stuber M, Kissinger KV, Salton CJ, Manning WJ. 2003. Cardiac structure and function in the obese: a cardiovascular magnetic resonance imaging study. J Cardiovasc Magn Reson 5:431-8

Datta SR, Brunet A, Greenberg ME. 1999. Cellular survival: a play in three Akts. Genes & development 13:2905-27

Deroanne CF, Lapiere CM, Nusgens BV. 2001. In vitro tubulogenesis of endothelial cells by relaxation of the coupling extracellular matrix-cytoskeleton. Cardiovascular research 49:647-58

Discher DE, Janmey P, Wang YL. 2005. Tissue cells feel and respond to the stiffness of their substrate. Science (New York, N.Y 310:1139-43

Dobereiner HG, Dubin-Thaler BJ, Giannone G, Sheetz MP. 2005. Force sensing and generation in cell phases: analyses of complex functions. J Appl Physiol 98:1542-6

Dormond O, Madsen JC, Briscoe DM. 2007. The effects of mTOR-Akt interactions on anti-apoptotic signaling in vascular endothelial cells. The Journal of biological chemistry 282:23679-86

Drangova M, Holdsworth DW, Boyd CJ, Dunmore PJ, Roach MR, Fenster A. 1993. Elasticity and geometry measurements of vascular specimens using a high-resolution laboratory CT scanner. Physiological measurement 14:277-90

Dufour C, Holy X, Marie PJ. 2008. Transforming growth factor-{beta} prevents osteoblast apoptosis induced by skeletal unloading via PI3K/Akt, Bcl-2, and phospho-Bad signaling. Am J Physiol Endocrinol Metab 294:E794-801

Eide BL, Turck CW, Escobedo JA. 1995. Identification of Tyr-397 as the primary site of tyrosine phosphorylation and pp60src association in the focal adhesion kinase, pp125FAK. Molecular and cellular biology 15:2819-27

Engler A, Bacakova L, Newman C, Hategan A, Griffin M, Discher D. 2004. Substrate compliance versus ligand density in cell on gel responses. Biophysical journal 86:617-28

Engler AJ, Griffin MA, Sen S, Bonnemann CG, Sweeney HL, Discher DE. 2004. Myotubes differentiate optimally on substrates with tissue-like stiffness: pathological implications for soft or stiff microenvironments. The Journal of cell biology 166:877-87

Engler AJ, Rehfeldt F, Sen S, Discher DE. 2007. Microtissue elasticity: measurements by atomic force microscopy and its influence on cell differentiation. Methods in cell biology 83:521-45

Engler AJ, Sen S, Sweeney HL, Discher DE. 2006. Matrix elasticity directs stem cell lineage specification. Cell 126:677-89

Engler AJ, Sweeney HL, Discher DE, Schwarzbauer JE. 2007. Extracellular matrix elasticity directs stem cell differentiation. Journal of musculoskeletal & neuronal interactions 7:335

Folkman J, Moscona A. 1978. Role of cell shape in growth control. Nature 273:345-9

Franchini KG, Torsoni AS, Soares PH, Saad MJ. 2000. Early activation of the multicomponent signaling complex associated with focal adhesion kinase induced by pressure overload in the rat heart. Circulation research 87:558-65

Franke TF, Kaplan DR, Cantley LC. 1997. PI3K: downstream AKTion blocks apoptosis. Cell 88:435-7

Frey MT, Engler A, Discher DE, Lee J, Wang YL. 2007. Microscopic methods for measuring the elasticity of gel substrates for cell culture: microspheres, microindenters, and atomic force microscopy. Methods in cell biology 83:47-65

Fujio Y, Walsh K. 1999. Akt mediates cytoprotection of endothelial cells by vascular endothelial growth factor in an anchorage-dependent manner. The Journal of biological chemistry 274:16349-54

Galbraith CG, Yamada KM, Sheetz MP. 2002. The relationship between force and focal complex development. The Journal of cell biology 159:695-705

Garcia AJ, Boettiger D. 1999. Integrin-fibronectin interactions at the cell-material interface: initial integrin binding and signaling. Biomaterials 20:2427-33

Garcia AJ, Takagi J, Boettiger D. 1998. Two-stage activation for alpha5beta1 integrin binding to surface-adsorbed fibronectin. The Journal of biological chemistry 273:34710-5

Garcia AJ, Vega MD, Boettiger D. 1999. Modulation of cell proliferation and differentiation through substrate-dependent changes in fibronectin conformation. Molecular biology of the cell 10:785-98

Georges PC, Janmey PA. 2005. Cell type-specific response to growth on soft materials. J Appl Physiol 98:1547-53

Ghajar CM, Chen X, Harris JW, Suresh V, Hughes CC, et al. 2008. The effect of matrix density on the regulation of 3-D capillary morphogenesis. Biophysical journal 94:1930-41

Ghosh K, Pan Z, Guan E, Ge S, Liu Y, et al. 2007. Cell adaptation to a physiologically relevant ECM mimic with different viscoelastic properties. Biomaterials 28:671-9

Giancotti FG, Ruoslahti E. 1999. Integrin signaling. Science (New York, N.Y 285:1028-32

Giannone G, Sheetz MP. 2006. Substrate rigidity and force define form through tyrosine phosphatase and kinase pathways. Trends in cell biology 16:213-23

Gimbrone MA, Jr. 1976. Culture of vascular endothelium. Progress in hemostasis and thrombosis 3:1-28

Guan JL. 1997. Focal adhesion kinase in integrin signaling. Matrix Biol 16:195-200

Guo WH, Frey MT, Burnham NA, Wang YL. 2006. Substrate rigidity regulates the formation and maintenance of tissues. Biophysical journal 90:2213-20

Ha CH, Bennett AM, Jin ZG. 2008. A novel role of vascular endothelial cadherin in modulating c-Src activation and downstream signaling of vascular endothelial growth factor. The Journal of biological chemistry 283:7261-70

Halliday NL, Tomasek JJ. 1995. Mechanical properties of the extracellular matrix influence fibronectin fibril assembly in vitro. Experimental cell research 217:109-17

Harris AK, Stopak D, Wild P. 1981. Fibroblast traction as a mechanism for collagen morphogenesis. Nature 290:249-51

Hay ED. 1981. Cell Biology of Extracellular Matrix. New York: Plenum Press
Hu G, Place AT, Minshall RD. 2008. Regulation of endothelial permeability by Src kinase signaling: vascular leakage versus transcellular transport of drugs and macromolecules. Chemico-biological interactions 171:177-89

Huang S, Chen CS, Ingber DE. 1998. Control of cyclin D1, p27(Kip1), and cell cycle progression in human capillary endothelial cells by cell shape and cytoskeletal tension. Molecular biology of the cell 9:3179-93

Ingber DE. 2002. Mechanical signaling and the cellular response to extracellular matrix in angiogenesis and cardiovascular physiology. Circulation research 91:877-87

Ingber DE, Folkman J. 1989. Mechanochemical switching between growth and differentiation during fibroblast growth factor-stimulated angiogenesis in vitro: role of extracellular matrix. The Journal of cell biology 109:317-30

Ingber DE, Prusty D, Frangioni JV, Cragoe EJ, Jr., Lechene C, Schwartz MA. 1990. Control of intracellular pH and growth by fibronectin in capillary endothelial cells. The Journal of cell biology 110:1803-11

Jalali S, del Pozo MA, Chen K, Miao H, Li Y, et al. 2001. Integrin-mediated mechanotransduction requires its dynamic interaction with specific extracellular matrix (ECM) ligands. Proceedings of the National Academy of Sciences of the United States of America 98:1042-6

Jalali S, Li YS, Sotoudeh M, Yuan S, Li S, et al. 1998. Shear stress activates p60src-Ras-MAPK signaling pathways in vascular endothelial cells. Arteriosclerosis, thrombosis, and vascular biology 18:227-34

Janmey PA, McCulloch CA. 2007. Cell mechanics: integrating cell responses to mechanical stimuli. Annual review of biomedical engineering 9:1-34

Janmey PA, Weitz DA. 2004. Dealing with mechanics: mechanisms of force transduction in cells. Trends in biochemical sciences 29:364-70

Jiang G, Huang AH, Cai Y, Tanase M, Sheetz MP. 2006. Rigidity sensing at the leading edge through alphavbeta3 integrins and RPTPalpha. Biophysical journal 90:1804-9

Juliano RL, Haskill S. 1993. Signal transduction from the extracellular matrix. The Journal of cell biology 120:577-85

Kobayashi-Sakamoto M, Isogai E, Hirose K, Chiba I. 2008. Role of alphav integrin in osteoprotegerin-induced endothelial cell migration and proliferation. Microvascular research 76:139-44

Kornberg LJ, Earp HS, Turner CE, Prockop C, Juliano RL. 1991. Signal transduction by integrins: increased protein tyrosine phosphorylation caused by clustering of beta 1 integrins. Proceedings of the National Academy of Sciences of the United States of America 88:8392-6

Kumar CC. 1998. Signaling by integrin receptors. Oncogene 17:1365-73

Kureishi Y, Luo Z, Shiojima I, Bialik A, Fulton D, et al. 2000. The HMG-CoA reductase inhibitor simvastatin activates the protein kinase Akt and promotes angiogenesis in normocholesterolemic animals. Nature medicine 6:1004-10

Kusaka K, Harihara Y, Torzilli G, Kubota K, Takayama T, et al. 2000. Objective evaluation of liver consistency to estimate hepatic fibrosis and functional reserve for hepatectomy. Journal of the American College of Surgeons 191:47-53

Labropoulos N, Ashraf Mansour M, Kang SS, Oh DS, Buckman J, Baker WH. 2000. Viscoelastic properties of normal and atherosclerotic carotid arteries. Eur J Vasc Endovasc Surg 19:221-5

Liao D, Arnett DK, Tyroler HA, Riley WA, Chambless LE, et al. 1999. Arterial stiffness and the development of hypertension. The ARIC study. Hypertension 34:201-6

Liu Y, Senger DR. 2004. Matrix-specific activation of Src and Rho initiates capillary morphogenesis of endothelial cells. Faseb J 18:457-68

Lo CM, Wang HB, Dembo M, Wang YL. 2000. Cell movement is guided by the rigidity of the substrate. Biophysical journal 79:144-52

MacLean NF, Dudek NL, Roach MR. 1999. The role of radial elastic properties in the development of aortic dissections. J Vasc Surg 29:703-10

Maher JJ, Friedman SL, Roll FJ, Bissell DM. 1988. Immunolocalization of laminin in normal rat liver and biosynthesis of laminin by hepatic lipocytes in primary culture. Gastroenterology 94:1053-62

McNamee HP, Liley HG, Ingber DE. 1996. Integrin-dependent control of inositol lipid synthesis in vascular endothelial cells and smooth muscle cells. Experimental cell research 224:116-22

Meredith JE, Jr., Fazeli B, Schwartz MA. 1993. The extracellular matrix as a cell survival factor. Molecular biology of the cell 4:953-61

Meredith JE, Jr., Winitz S, Lewis JM, Hess S, Ren XD, et al. 1996. The regulation of growth and intracellular signaling by integrins. Endocrine reviews 17:207-20

Montesano R, Orci L, Vassalli P. 1983. In vitro rapid organization of endothelial cells into capillary-like networks is promoted by collagen matrices. The Journal of cell biology 97:1648-52

Munevar S, Wang YL, Dembo M. 2001. Distinct roles of frontal and rear cell-substrate adhesions in fibroblast migration. Molecular biology of the cell 12:3947-54

Nagaraj A, Kim H, Hamilton AJ, Mun JH, Smulevitz B, et al. 2005. Porcine carotid arterial material property alterations with induced atheroma: an in vivo study. Medical engineering & physics 27:147-56

Nathan C, Sporn M. 1991. Cytokines in context. The Journal of cell biology 113:981-6

Oudit GY, Sun H, Kerfant BG, Crackower MA, Penninger JM, Backx PH. 2004. The role of phosphoinositide-3 kinase and PTEN in cardiovascular physiology and disease. Journal of molecular and cellular cardiology 37:449-71

Pajalunga D, Mazzola A, Franchitto A, Puggioni E, Crescenzi M. 2008. The logic and regulation of cell cycle exit and reentry. Cell Mol Life Sci 65:8-15

Pang PH, Lin YH, Lee YH, Hou HH, Hsu SP, Juan SH. 2008. Molecular mechanisms of p21 and p27 induction by 3-methylcholanthrene, an aryl-hydrocarbon receptor agonist, involved in antiproliferation of human umbilical vascular endothelial cells. Journal of cellular physiology 215:161-71

Pelham RJ, Jr., Wang Y. 1997. Cell locomotion and focal adhesions are regulated by substrate flexibility. Proceedings of the National Academy of Sciences of the United States of America 94:13661-5

Pelham RJ, Jr., Wang YL. 1998. Cell locomotion and focal adhesions are regulated by the mechanical properties of the substrate. The Biological bulletin 194:348-9; discussion 9-50

Peyton SR, Ghajar CM, Khatiwala CB, Putnam AJ. 2007. The emergence of ECM mechanics and cytoskeletal tension as important regulators of cell function. Cell biochemistry and biophysics 47:300-20

Peyton SR, Kim PD, Ghajar CM, Seliktar D, Putnam AJ. 2008. The effects of matrix stiffness and RhoA on the phenotypic plasticity of smooth muscle cells in a 3-D biosynthetic hydrogel system. Biomaterials 29:2597-607

Peyton SR, Putnam AJ. 2005. Extracellular matrix rigidity governs smooth muscle cell motility in a biphasic fashion. Journal of cellular physiology 204:198-209

Peyton SR, Raub CB, Keschrumrus VP, Putnam AJ. 2006. The use of poly(ethylene glycol) hydrogels to investigate the impact of ECM chemistry and mechanics on smooth muscle cells. Biomaterials 27:4881-93

Reiske HR, Kao SC, Cary LA, Guan JL, Lai JF, Chen HC. 1999. Requirement of phosphatidylinositol 3-kinase in focal adhesion kinase-promoted cell migration. The Journal of biological chemistry 274:12361-6

Rice DC, Dobrian AD, Schriver SD, Prewitt RL. 2002. Src autophosphorylation is an early event in pressure-mediated signaling pathways in isolated resistance arteries. Hypertension 39:502-7

Ross R. 1999. Atherosclerosis--an inflammatory disease. The New England journal of medicine 340:115-26

Sanders M. 1994. Molecular and cellular concepts in atherosclerosis. Pharmacology & therapeutics 61:109-53

Sawada Y, Tamada M, Dubin-Thaler BJ, Cherniavskaya O, Sakai R, et al. 2006. Force sensing by mechanical extension of the Src family kinase substrate p130Cas. Cell 127:1015-26

Schwartz MA, Assoian RK. 2001. Integrins and cell proliferation: regulation of cyclin-dependent kinases via cytoplasmic signaling pathways. Journal of cell science 114:2553-60

Schwartz MA, Lechene C, Ingber DE. 1991. Insoluble fibronectin activates the Na/H antiporter by clustering and immobilizing integrin alpha 5 beta 1, independent of cell shape. Proceedings of the National Academy of Sciences of the United States of America 88:7849-53

Schwartz SM, Ross R. 1984. Cellular proliferation in atherosclerosis and hypertension. Progress in cardiovascular diseases 26:355-72

Sheetz MP. 1994. Cell migration by graded attachment to substrates and contraction. Seminars in cell biology 5:149-55

Sheetz MP, Felsenfeld D, Galbraith CG, Choquet D. 1999. Cell migration as a five-step cycle. Biochemical Society symposium 65:233-43

Sheetz MP, Felsenfeld DP, Galbraith CG. 1998. Cell migration: regulation of force on extracellular-matrix-integrin complexes. Trends in cell biology 8:51-4

Shiojima I, Walsh K. 2002. Role of Akt signaling in vascular homeostasis and angiogenesis. Circulation research 90:1243-50

Sieminski AL, Hebbel RP, Gooch KJ. 2004. The relative magnitudes of endothelial force generation and matrix stiffness modulate capillary morphogenesis in vitro. Experimental cell research 297:574-84

Sneddon IN. 1965. The relation between load and penetration in the axisymmetric boussinesq problem for a punch of arbitrary profile. International Journal of Engineering Science 3:47-57

Stromblad S, Cheresh DA. 1996. Integrins, angiogenesis and vascular cell survival. Chemistry & biology 3:881-5

Thomas SM, Brugge JS. 1997. Cellular functions regulated by Src family kinases. Annual review of cell and developmental biology 13:513-609

Thyberg J. 1998. Phenotypic modulation of smooth muscle cells during formation of neointimal thickenings following vascular injury. Histology and histopathology 13:871-91

Thyberg J, Blomgren K, Hedin U, Dryjski M. 1995. Phenotypic modulation of smooth muscle cells during the formation of neointimal thickenings in the rat carotid artery after balloon injury: an electron-microscopic and stereological study. Cell and tissue research 281:421-33

Urbich C, Dernbach E, Reissner A, Vasa M, Zeiher AM, Dimmeler S. 2002. Shear stress-induced endothelial cell migration involves integrin signaling via the fibronectin receptor subunits alpha(5) and beta(1). Arteriosclerosis, thrombosis, and vascular biology 22:69-75

Vailhe B, Ronot X, Tracqui P, Usson Y, Tranqui L. 1997. In vitro angiogenesis is modulated by the mechanical properties of fibrin gels and is related to alpha(v)beta3 integrin localization. In vitro cellular & developmental biology 33:763-73

Vernon RB, Angello JC, Iruela-Arispe ML, Lane TF, Sage EH. 1992. Reorganization of basement membrane matrices by cellular traction promotes the formation of cellular networks in vitro. Laboratory investigation; a journal of technical methods and pathology 66:536-47

Vogel V, Sheetz M. 2006. Local force and geometry sensing regulate cell functions. Nature reviews 7:265-75

von Wichert G, Jiang G, Kostic A, De Vos K, Sap J, Sheetz MP. 2003. RPTP-alpha acts as a transducer of mechanical force on alphav/beta3-integrin-cytoskeleton linkages. The Journal of cell biology 161:143-53

Wallace CS, Strike SA, Truskey GA. 2007. Smooth muscle cell rigidity and extracellular matrix organization influence endothelial cell spreading and adhesion formation in coculture. American journal of physiology 293:H1978-86

Wang Y, Jin G, Miao H, Li JY, Usami S, Chien S. 2006. Integrins regulate VE-cadherin and catenins: dependence of this regulation on Src, but not on Ras. Proceedings of the National Academy of Sciences of the United States of America 103:1774-9

Westhoff MA, Serrels B, Fincham VJ, Frame MC, Carragher NO. 2004. SRC-mediated phosphorylation of focal adhesion kinase couples actin and adhesion dynamics to survival signaling. Molecular and cellular biology 24:8113-33

Wong JY, Velasco, A., Rajagopalan, P., and Pham, Q. 2003. Directed movement of vascular smooth muscle cells on gradient-compliant hydrogels. Langmuir 19:1908-13

Wuyts FL, Vanhuyse VJ, Langewouters GJ, Decraemer WF, Raman ER, Buyle S. 1995. Elastic properties of human aortas in relation to age and atherosclerosis: a structural model. Physics in medicine and biology 40:1577-97

Yang S, Graham J, Kahn JW, Schwartz EA, Gerritsen ME. 1999. Functional roles for PECAM-1 (CD31) and VE-cadherin (CD144) in tube assembly and lumen formation in three-dimensional collagen gels. The American journal of pathology 155:887-95

Yeung T, Georges PC, Flanagan LA, Marg B, Ortiz M, et al. 2005. Effects of substrate stiffness on cell morphology, cytoskeletal structure, and adhesion. Cell motility and the cytoskeleton 60:24-34

Zhao J, Pestell R, Guan JL. 2001. Transcriptional activation of cyclin D1 promoter by FAK contributes to cell cycle progression. Molecular biology of the cell 12:4066-77

Zhao JH, Guan JL. 2000. Role of focal adhesion kinase in signaling by the extracellular matrix. Progress in molecular and subcellular biology 25:37-55

Zhao JH, Reiske H, Guan JL. 1998. Regulation of the cell cycle by focal adhesion kinase. The Journal of cell biology 143:1997-2008